8-25-2022

Comprehensive Review of Heat Transfer Correlations of Supercritical CO2 in Straight Tubes Near the Critical Point: A Historical Perspective

Nicholas C. Lopes
Embry-Riddle Aeronautical University, lopesn2@my.erau.edu

Yang Chao
Embry-Riddle Aeronautical University, chaoy@my.erau.edu

Vinusha Dasarla
Embry-Riddle Aeronautical University, DASARLAV@my.erau.edu

Neil P. Sullivan
Embry-Riddle Aeronautical University, SULLIVN6@erau.edu

Mark Ricklick
Embry-Riddle Aeronautical University, ridlickm@erau.edu

See next page for additional authors

Scholarly Commons Citation
Lopes, N. C., Chao, Y., Dasarla, V., Sullivan, N. P., Ricklick, M., & Boetcher, S. (2022). Comprehensive Review of Heat Transfer Correlations of Supercritical CO2 in Straight Tubes Near the Critical Point: A Historical Perspective. *Journal of Heat and Mass Transfer,* (). https://doi.org/10.1115/1.4055345

Authors

Nicholas C. Lopes, Yang Chao, Vinusha Dasarla, Neil P. Sullivan, Mark Ricklick, and Sandra Boetcher

Journal of Heat Transfer. Received April 07, 2022;
Accepted manuscript posted August 25, 2022. doi:10.1115/1.4055345

Comprehensive Review of Heat Transfer Correlations of Supercritical CO_2 in Straight Tubes Near the Critical Point: A Historical Perspective

Nicholas C. Lopes[1], Yang Chao[1], Vinusha Dasarla[2], Neil P. Sullivan[3], Mark A. Ricklick[2], and Sandra K. S. Boetcher[1,4,*]

[1]Department of Mechanical Engineering
Embry-Riddle Aeronautical University
Daytona Beach, FL USA 32114

[2]Department of Aerospace Engineering
Embry-Riddle Aeronautical University
Daytona Beach, FL USA 32114

[3]Department of Mechanical Engineering
Embry-Riddle Aeronautical University
Prescott, AZ USA 86301

[4]Fellow ASME

[*]Corresponding Author: sandra.boetcher@erau.edu

ABSTRACT

An exhaustive review was undertaken to assemble all available correlations for supercritical CO_2 in straight, round tubes of any orientation with special attention paid to how the wildly varying fluid properties near the critical point are handled. The assemblage of correlations, and subsequent discussion, is presented from a historical perspective, starting from pioneering work on the topic in the 1950s to the modern day. Despite the growing sophistication of sCO_2 heat transfer correlations, modern correlations are still only generally applicable over a relatively small range of operating conditions, and there has not been a substantial increase in predictive capabilities. Recently, researchers have turned to machine learning as a tool for next-generation heat transfer prediction. An overview of the state-of-the-art of predicting sCO_2 heat transfer using machine learning methods, such as artificial neural networks, is also presented.

Journal of Heat Transfer. Received April 07, 2022;
Accepted manuscript posted August 25, 2022. doi:10.1115/1.4055345

Nomenclature

A	Function
Ac	Acceleration parameter
B	Coefficient
Bu	Buoyancy parameter
C	Coefficient
c	Specific heat [J/(kg·K)]
c_p	Specific heat at constant pressure [J/(kg·K)]
$\overline{c}_p$	Integrated specific heat at constant pressure $= \frac{1}{T_w - T_b} \int_{T_b}^{T_w} c_p \, dT$ [J/(kg·K)]
d	Inside tube diameter [m]
G	Mass flux [kg/(m^2·s)]
Gr	Grashof number $= \frac{(\rho_b - \rho_w)\rho g d^3}{\mu^2}$
$\overline{Gr}$	Grashof number based on $\overline{\rho}$, $= \frac{(\rho_b - \overline{\rho})\rho g d^3}{\mu^2}$
Gr_q	Grashof number based on q, $= \frac{g\beta d^4 q}{\nu^2 k}$
$\overline{Gr}_q$	Grashof number based on q and $\overline{\beta}$, $= \frac{g\overline{\beta} d^4 q}{\nu^2 k}$
g	Acceleration due to gravity [m/s^2]
h	Specific enthalpy [J/kg]
K	Coefficient or parameter
k	Thermal conductivity [W/(m·K)]
$\overline{k}$	Integrated thermal conductivity $= \frac{1}{T_w - T_b} \int_{T_b}^{T_w} k \, dT$ [kg/m^3]
l	Heated/cooled tube length [m]
m	Exponent
$\dot{m}$	Mass flow rate [kg/s]
n	Exponent
Nu	Nusselt number
Nu_0	Reference Nusselt number
P	Pressure [Pa]
Pr	Prandtl number $= \frac{\mu c_p}{k}$
$\overline{Pr}$	Prandtl number based on $\overline{c}_p$, $= \frac{\mu \overline{c}_p}{k}$
$\overline{\overline{Pr}}$	Integrated Prandtl number $= \frac{1}{T_w - T_b} \int_{T_b}^{T_w} Pr(T) dT$
q	Wall heat flux [W/m^2]
q^+	Non-dimensional wall heat flux $= \frac{q\beta}{G c_p}$
Re	Reynolds number $= \frac{dG}{\mu}$
$\overline{Re}$	Integrated Reynolds number $= \frac{dG}{T_w - T_b} \int_{T_b}^{T_w} \frac{dT}{\mu(T)}$
Ri	Richardson number $= \frac{Gr}{Re_b^2}$
T	Temperature [K]
V	Velocity [m/s]
v	Specific volume [m^3/kg]
x	Axial distance from tube inlet [m]

Journal of Heat Transfer. Received April 07, 2022;
Accepted manuscript posted August 25, 2022. doi:10.1115/1.4055345

Greek

α	Heat transfer coefficient [W/(m^2·K)]
β	Volume expansion coefficient $= \frac{-1}{\rho}(\frac{\partial \rho}{\partial T})_P$ [1/K]
$\overline{\beta}$	Volume expansion coefficient based on $\overline{\rho}$, $= \frac{-1}{\overline{\rho}}(\frac{\partial \rho}{\partial T})_P$ [1/K]
ϵ	Tube wall roughness [m]
μ	Dynamic viscosity [Pa·s]
$\overline{\mu}$	Integrated dynamic viscosity $= \frac{1}{T_w - T_b} \int_{T_b}^{T_w} \mu \, dT$ [Pa·s]
ν	Kinematic viscosity $= \frac{\mu}{\rho}$ [m^2/s]
ξ	Friction factor
ρ	Density [kg/m^3]
$\overline{\rho}$	Integrated density $= \frac{1}{T_w - T_b} \int_{T_b}^{T_w} \rho \, dT$ [kg/m^3]
τ	Shear stress [Pa]
ϕ	Length correcting factor
φ	Correcting factor

Subscripts

b	Bulk
c	Critical
f	Film
in	Inlet
pc	Pseudocritical
out	Outlet
w	Wall

Journal of Heat Transfer. Received April 07, 2022;
Accepted manuscript posted August 25, 2022. doi:10.1115/1.4055345

1 Introduction

Supercritical carbon dioxide (sCO_2) is used in a wide range of industries [1–3] for refrigeration [4], power generation [5–9], and thermal management [10]. Near its critical point (P = 7.38 MPa and T = 31.0 °C), carbon dioxide is an excellent heat transfer fluid due to the very high specific heat (see Fig. 1). The steep thermophysical property gradients observed near the critical point, along the pseudocritical line, cause the heat transfer coefficients to depart significantly from those determined from conventional Nusselt number correlations for subcritical flow. In fact, small uncertainties in property data, which are exacerbated from the large gradients near the pseudocritical line, can result in very high uncertainties in heat transfer coefficients [11]. Although there is no official set region defined as "near-critical," generally, heat transfer coefficient prediction issues occur for pressures between 7.38 MPa and 9 MPa, and temperature ranges between 30 °C and 50 °C, with the most significant departures from conventional correlations occurring between 7.38 MPa and 8 MPa and temperatures between 30 °C and 40 °C.

Furthermore, for supercritical fluids, it is difficult to define an appropriate reference thermal conductivity and specific heat since they vary greatly near the pseudocritical point, adding difficulty to the Nusselt number calculations. Due to the difficulty in defining a reference thermal conductivity and specific heat, much of the experimental and numerical sCO_2 literature reports only the dimensional heat transfer coefficient. The sensitivity of these parameters and their effect on the Nusselt number could also explain the myriad of attempts to correlate sCO_2 data, with no single correlation to date being able to accurately predict Nusselt numbers over a wide array of operating conditions. Nonetheless, in an attempt to provide predictive capabilities, many researchers have modified subcritical Nusselt number correlations so that they are applicable to supercritical fluids.

There are several review articles on sCO_2 heat transfer correlations pertaining to tubular geometries, and attempts have been made to determine the best correlation for predicting sCO_2 thermal behavior. Pitla et al. [12] reviewed heat transfer and pressure drop correlations for sCO_2 in horizontal and vertical tubes under both heating and cooling conditions. The correlations developed for cooling were compared against one another. Pioro et al. [13] surveyed supercritical heat transfer correlations, primarily for water, carbon dioxide, and helium in tubular geometries. Several selected correlations were compared, and the results showed significant differences in calculated heat transfer coefficient values. Duffey and Pioro [14] reviewed sCO_2 correlations in (primarily) tubes of vertical and horizontal orientation, noting that limited attention was being placed on other flow geometries up to that point. It was found three possible heat transfer regimes (normal, deteriorated, and enhanced) are achievable under different flow orientations and conditions. Cheng et al. [15] reported and compared available sCO_2 heat transfer and pressure drop correlations in

Journal of Heat Transfer. Received April 07, 2022;
Accepted manuscript posted August 25, 2022. doi:10.1115/1.4055345

macro- and micro-tube geometries under cooling conditions. A comment was given on the lack of pertinent experimental details required to properly utilize most data from the literature to correlate sCO_2 heat transfer data. Fang and Xu [16] provided a review of heat transfer correlations for in-tube cooling of sCO_2. The correlations were directly compared using experimental data from the available literature, and a new correlation was developed. Lin et al. [17] compared existing heat transfer correlations for sCO_2 in horizontal tubes under cooling conditions. It was found that most of the correlations agreed well with the experimental data of Dang and Hihara [18] at low heat fluxes, but fail to do so at high heat fluxes. Cabeza et al. [19] reviewed available sCO_2 experimental studies, heat transfer correlations of various geometries, and applications as a heat transfer fluid. The review showed a lack of a universal correlation, for each geometry, describing heat transfer trends over a wide array of operating conditions. Ehsan et al. [20] reviewed heat transfer and friction factor correlations for sCO_2 in horizontal and vertical tubes under both heating and cooling conditions. Ehsan et al. [20] cited sensitivity to tube diameter, mass flux, heat flux, and operating pressure on heat transfer coefficient as reasons for the applicability limitations of individual correlation. Fan et al. [21] performed a review on existing sCO_2 heat transfer correlations in tubes under uniform heating conditions. A comparison was made between several correlations (including the one developed in the paper [21]) using experimental data from the literature. Xie et al. [22] reviewed heat transfer deterioration of sCO_2 in vertical tubes and heat transfer correlations of sCO_2 in tubes of both horizontal and vertical orientation. Bodkha and Maheshwari [23] reviewed supercritical heat transfer correlations in tubes, primarily for water and CO_2. A detailed comparison of heat transfer coefficients from each correlation was provided using several experimental datasets from the literature.

Many of these review articles are either focused on applications, one or more specific types of geometries, heating or cooling, a specific flow direction, or some other niche area. The purpose of the present manuscript is to provide a comprehensive collection and discussion of all Nusselt number correlations for sCO_2 in tubes developed by various investigators from a historical perspective, with an emphasis on the different ways in which the property variations were addressed in the particular correlations. As seen in the subsequent text, most, if not all, of these types of correlations are for the Nusselt number; although, as previously discussed, determining an appropriate reference thermal conductivity and specific heat is a challenge. As will be discussed, despite the large efforts in the last decade and the plethora of sCO_2 correlations produced, there has not been a substantial increase in predictive capabilities. Furthermore, many modern correlations are generally only applicable under relatively small ranges of operating conditions and flow orientations. Recently, researchers have turned to artificial neural networks (ANN), a subset of machine learning (ML), to develop potentially more accurate ways of predicting heat transfer coefficients

Journal of Heat Transfer. Received April 07, 2022;
Accepted manuscript posted August 25, 2022. doi:10.1115/1.4055345

without having to worry about a dimensionless correlation. A review of recent advances in ML to predict sCO_2 heat transfer is also presented.

2 1950s - 1960s (Early Investigators)

In the 1950s, the use of supercritical water (sH_2O) as the working fluid in fossil fuel power plants became an attractive idea for increasing their thermal efficiency. Additionally, in the late 1950s through the 1960s, a potential application of supercritical fluids as coolants for nuclear reactors was explored by the USA and USSR, with sH_2O being a primary candidate [13]. However, the high critical temperature and pressure of sH_2O motivated the use of sCO_2 in several early fundamental investigations due to its significantly milder critical point. For each correlation presented in this section, information on type of boundary condition(s), flow direction(s), and operating conditions is found in Table 6.

In 1957, Bringer and Smith [24] experimentally investigated horizontal flow of sCO_2 in a tube under uniform heating and developed the following local heat transfer correlation

$$Nu = C\, Re_x^{0.77}\, Pr_w^{0.55} \tag{1}$$

where $C = 0.0266$ for sH_2O and $C = 0.0375$ for sCO_2. The properties within the Reynolds number, Re_x, were evaluated at T_x, the characteristic temperature, defined as

$$T_x = \begin{cases} T_b & \text{if } \frac{T_{pc}-T_b}{T_w-T_b} < 0 \\ T_{pc} & \text{if } 0 \leq \frac{T_{pc}-T_b}{T_w-T_b} \leq 1 \\ T_w & \text{if } \frac{T_{pc}-T_b}{T_w-T_b} > 1 \end{cases} \tag{2}$$

The use of different reference temperatures to evaluate the Reynolds number was not a common approach taken by subsequent investigators. Often times, as will be presented, authors selected a single reference temperature to evaluate most, if not all, properties in their heat transfer correlations. However, a few investigators in the mid 2010s [25, 26] also examined the effects of wall, bulk, and film ($\frac{T_w+T_b}{2}$) reference temperatures in their correlations, similar to Bringer and Smith [24].

Using available experimental data from the literature, Petukhov and Kirillov [27] developed the following local heat transfer correlation in 1958 for subcritical turbulent fluids in smooth horizontal tubes.

Journal of Heat Transfer. Received April 07, 2022;
Accepted manuscript posted August 25, 2022. doi:10.1115/1.4055345

$$Nu = Nu_0 \left(\frac{\mu_w}{\mu_b}\right)^{-n} \quad (3)$$

where $n = 0.11$ for heating and $n = 0.25$ for cooling. They defined Nu_0 as

$$Nu_0 = \frac{(\xi/8)\, Re\, Pr}{1.07 + 12.7\sqrt{\xi/8}\,(Pr^{2/3} - 1)} \quad (4)$$

The friction factor ξ is calculated using the Filonenko correlation [28]

$$\xi = \frac{1}{(1.82\, log_{10}(Re)\; - 1.64)^2} \quad (5)$$

Nu_0 and ξ are evaluated using bulk properties.

Petukhov and Kirillov [27] stated that heat transfer for turbulent flow in tubes may be sufficiently approximated using a combination of the following criterion

$$Nu_b = f\left(Re_b,\, Pr_b,\, \frac{\mu_w}{\mu_b},\, \frac{k_w}{k_b},\, \frac{c_{p,w}}{c_{p,b}},\, \frac{\rho_w}{\rho_b}\right) \quad (6)$$

The functional dependence of heat transfer on these parameters is derived in Jackson and Hall [29] using dimensional analysis. For the range of experimental conditions used in their study, Petukhov and Kirillov [27] determined there was significant variation in only fluid viscosity, while other physical parameters (thermal conductivity, specific heat, and density) changed within relatively narrow margins. As a result, they combined Eq. (4) with a viscosity property ratio (or viscosity correcting factor) μ_w/μ_b into their final correlation, Eq. (3). The former equation was a generalized correlation derived under the assumption of constant physical properties of the fluid, and the latter was added to account for the effect of viscosity variations with local temperature gradients on heat transfer. Utilizing wall-to-bulk physical property ratios raised to suitable powers as 'correcting factors' in heat transfer correlations, where local physical properties vary significantly in the span-wise direction with temperature, was not a new concept in the late 1950s. However, this technique is extremely common in formulating sCO_2 heat transfer correlations, where physical properties are subject to high variations, so it is worth noting here.

The expression for Nu_0 (Eq. (4)), known as the Petukhov and Kirillov correlation, was derived semi-empirically, with the constants 1.07 and 12.7 in the denominator being curve-fitted with the available experimental data. The correlation takes a similar form to earlier correlations developed by Prandtl, Taylor, and von Kármán (to name a few) relating heat transfer and friction in tubes, discussed to some extent in [30–33]. Though not the first of this form, and despite it being

Journal of Heat Transfer. Received April 07, 2022;
Accepted manuscript posted August 25, 2022. doi:10.1115/1.4055345

originally developed for subcritical fluids, the Petukhov and Kirillov correlation (Eq. (4)) has been applied extensively in many subsequent studies of sCO_2.

A common misconception about the Petukhov and Kirillov correlation (Eq. (4)) in the present day is the use of $\overline{Pr}$, the Prandtl number based on integrated specific heat $\bar{c}_p$ (both of which are defined in the Nomenclature), in the numerator. An inspection of the original 1958 paper yields no indication of the use of $\overline{Pr}$ or $\bar{c}_p$; the Prandtl number was simply evaluated using exclusively bulk properties. In fact, $\bar{c}_p$ was not introduced to correlations involving sCO_2 until Krasnoshchekov and Protopopov [34] in 1960, and $\overline{Pr}$ likewise was not introduced to correlations involving sCO_2 until Swenson et al. [35] in 1965.

In 1960, Krasnoshchekov and Protopopov [34], using available experimental data from the literature, developed the following local heat transfer correlation for sH_2O and sCO_2 in horizontal tubes under uniform heating

$$Nu = Nu_0 \left(\frac{\mu_b}{\mu_w}\right)^{0.11} \left(\frac{k_b}{k_w}\right)^{-0.33} \left(\frac{\bar{c}_p}{c_{p,b}}\right)^{0.35} \tag{7}$$

where Nu_0 is the Petukhov and Kirillov correlation (Eq. (4)), which evaluates ξ using the Filonenko correlation (Eq. (5)). Both Nu_0 and ξ are evaluated using bulk properties.

Krasnoshchekov and Protopopov [34] further developed the correcting factors over a broader range of operating conditions by introducing the integrated specific heat $\bar{c}_p$ (defined in the Nomenclature) within the specific heat correcting factor. As alluded to earlier, the large variations of physical properties with local temperature gradients makes it difficult to evaluate these properties at a single temperature (e.g., wall, bulk, or film) with reasonable accuracy. Thus, the introduction of a specific heat that was integrated from the bulk to the wall temperatures was deemed more suitable.

It is worth noting that Eq. (7) also appears in the more detailed work of Petukhov et al. [36], published in 1961 by the same authors of [34]. The 1961 paper expands on the derivation of Eq. (7) and more formally introduces the integrated specific heat. In the literature, Eq. (7) is often credited to some combination of the two papers.

In 1963, Petukhov and Popov [37] generalized (and increased the accuracy of) the Petukhov and Kirillov correlation (Eq. (4)) for a larger spread of experimental data by expanding the constants 1.07 and 12.7 in the denominator to functions of ξ and Pr, respectively, as follows

$$Nu = \frac{(\xi/8)\, Re\, Pr}{k_1(\xi) + k_2(Pr)\sqrt{\xi/8}\,(Pr^{2/3} - 1)} \tag{8}$$

where

Journal of Heat Transfer. Received April 07, 2022;
Accepted manuscript posted August 25, 2022. doi:10.1115/1.4055345

$$k_1\left(\xi\right) = 1 + 3.4\xi \tag{9}$$

$$k_2\left(Pr\right) = 11.7 + 1.8\,Pr^{-1/3} \tag{10}$$

ξ is calculated using the Filonenko correlation Eq. (5); Nu and ξ are evaluated using bulk properties. The correlation is valid for subcritical, turbulent fluids in smooth tubes.

In 1965, Swenson et al. [35] experimentally investigated upward flow of sH_2O in a tube under uniform heating and developed the following correlation for local heat transfer of sH_2O and sCO_2

$$Nu = 0.00459\,Re_w^{0.923}\,\overline{Pr}_w^{\,0.613}\left(\frac{v_b}{v_w}\right)^{0.231} \tag{11}$$

Here, v is specific volume. As previously mentioned, Swenson et al. [35] were the first to implement $\overline{Pr}$, the Prandtl number based on $\bar{c}_p$, in an sCO_2 heat transfer correlation. The parameter $\overline{Pr}$, as defined in the Nomenclature, is evaluated using $\bar{c}_p$ to account for specific heat variations due to local temperature gradients.

Krasnoshchekov and Protopopov [38], in 1966, performed experiments regarding horizontal flow of sCO_2 in a tube under uniform heating and developed the following local heat transfer correlation

$$Nu = Nu_0\left(\frac{\rho_w}{\rho_b}\right)^{0.3}\left(\frac{\bar{c}_p}{c_{p,b}}\right)^{n} \tag{12}$$

where Nu_0 is the Petukhov and Kirillov correlation (Eq. (4)), which evaluates ξ using the Filonenko correlation (Eq. (5)). Both Nu_0 and ξ are evaluated using bulk properties. They determined that the exponent n of the specific heat correcting factor is a function of T_w/T_{pc} and T_b/T_{pc}. The relationship for n was provided graphically and is shown in Fig. 2. The correlation takes a similar form to Eq. (7) from their earlier work [34, 36], where the Petukhov and Kirillov correlation (Eq. (4)) is expanded to include correcting factors and the integrated specific heat.

3 1970s - 1980s

For each correlation presented in this section, information on type of boundary condition(s), flow direction(s), and operating conditions is found in Table 7. Krasnoshchekov et al. [39] experimentally investigated horizontal flow of sCO_2 in a tube-in-tube heat exchanger, cooled by water in the annulus, in 1970. They were the first to explicitly correlate local sCO_2 cooling data, as opposed

Journal of Heat Transfer. Received April 07, 2022;
Accepted manuscript posted August 25, 2022. doi:10.1115/1.4055345

to prior investigators only using heating data. The local heat transfer correlation is given as

$$Nu = Nu_0 \left(\frac{\rho_w}{\rho_b}\right)^n \left(\frac{\bar{c}_p}{c_{p,w}}\right)^m \tag{13}$$

where Nu_0 is the Petukhov and Kirillov correlation (Eq. (4)), which evaluates ξ using the Filonenko correlation (Eq. (5)). Unlike previous implementations of the Petukhov and Kirillov correlation (Eq. (4)), here, Nu_0 and ξ are evaluated using wall properties as it better correlated the data. The exponent m itself is a function of the specific heat correcting factor and is defined as

$$m = B \left(\frac{\bar{c}_p}{c_{p,w}}\right)^k \tag{14}$$

where n (not to be confused with n in Eq. (12)), B, and k (not to be confused with thermal conductivity) are functions of P/P_c and provided in Table 1.

In 1972, Krasnoshchekov and Protopopov [40] modified Eq. (12) from their previous work in 1966 regarding horizontal flow of sCO_2 in a tube under uniform heating. They made the correlation applicable over a larger pressure range by implementing a variable exponent on the density correcting factor as a function of pressure. Their modified correlation for local heat transfer is given as

$$Nu = Nu_0 \left(\frac{\bar{c}_p}{c_{p,b}}\right)^n \left(\frac{\rho_w}{\rho_b}\right)^m \tag{15}$$

where

$$m = 0.35 - 0.05 \left(\frac{P}{P_c}\right) \tag{16}$$

where Nu_0 is the Petukhov and Kirillov correlation (Eq. (4)), which evaluates ξ using the Filonenko correlation (Eq. (5)). Both Nu_0 and ξ are evaluated using bulk properties. The exponent n is determined graphically by Fig. 2. The correlation is valid under the same conditions as Eq. (12), with the exception of pressure (new applicable range is provided in Table 7. At pressures close to the critical pressure, the authors noted that Eq. (15) becomes Eq. (12).

Still in 1972, Krasnoshchekov et al. [41] again modified Eq. (12) from their previous work. This time, however, they incorporated a non-dimensional length factor accounting for thermal development near the tube entrance. The resulting correlation for local heat transfer is as follows

$$Nu = Nu_0 \left(\frac{\bar{c}_p}{c_{p,b}}\right)^n \left(\frac{\rho_w}{\rho_b}\right)^{0.3} f\left(\frac{x}{d}\right) \tag{17}$$

Journal of Heat Transfer. Received April 07, 2022;
Accepted manuscript posted August 25, 2022. doi:10.1115/1.4055345

where

$$f\left(\frac{x}{d}\right) = \begin{cases} 1 & \text{for } x/d > 15 \\ 0.95 + 0.95\left(\frac{d}{x}\right)^{0.8} & \text{for } 2 \le x/d \le 15 \end{cases} \tag{18}$$

and Nu_0 is the Petukhov and Kirillov correlation (Eq. (4)), which evaluates ξ using the Filonenko correlation (Eq. (5)). Both Nu_0 and ξ are evaluated using bulk properties. The exponent n is determined graphically by Fig. 2.

In 1973, Petukhov et al. [42] generalized the Petukhov and Kirillov correlation (Eq. (4)) for a larger spread of data by expanding the constant 1.07 in the denominator to a function of Re and Pr. The approach was very similar to that of Petukhov and Popov [37] reported in 1963. The modified correlation is as follows

$$Nu_0 = \frac{(\xi/8)\, Re\, Pr}{k + 12.7\sqrt{\xi/8}\,(Pr^{2/3} - 1)} \tag{19}$$

where

$$k = 1.07 + \frac{900}{Re} - \frac{0.63}{1 + 10\, Pr} \tag{20}$$

and the friction factor ξ is calculated as

$$\xi = \begin{cases} (1.82\, log_{10}(Re/8))^{-2} & \text{for } Re > 10^4 \\ \frac{0.3164}{Re^{1/4}} & \text{for } Re < 10^4 \end{cases} \tag{21}$$

It should be noted that the authors did not explicitly specify at what temperature (wall, bulk, or film) Nu and ξ should be evaluated. Petukhov et al. [42] then modified Eq. (19) by adding correcting factors to account for local physical property variations as follows

$$Nu = Nu_0 \left(\frac{k_w}{k_b}\right)^{1/3} \left(\frac{c_{p,w}}{c_{p,b}}\right)^{1/4} \left(\frac{T_w}{T_b}\right)^{-\left(0.53 + \phi\left(\frac{x}{d}\right) log\left(\frac{\mu_w}{\mu_b}\right)\right)} \tag{22}$$

where the term $\phi\,(x/d)$ is a length correcting factor whose ranges are provided in Table 2.

In 1976, Gnielinski [32] modified Eq. (19) by Petukhov et al. [42] to better predict heat transfer of subcritical fluids in tubes over the transition range $Re = 2300 - 10^4$. The modified equation is as follows

$$Nu = \frac{(\xi/8)\,(Re - 1000)\, Pr}{1 + 12.7\sqrt{\xi/8}\,(Pr^{2/3} - 1)} \tag{23}$$

Journal of Heat Transfer. Received April 07, 2022;
Accepted manuscript posted August 25, 2022. doi:10.1115/1.4055345

In the same work, Gnielinski [32] modified their own correlation to account for the effects of tube length and local temperature-dependent properties on heat transfer

$$Nu = \frac{(\xi/8)\,(Re - 1000)\,Pr}{1 + 12.7\,\sqrt{\xi/8}\,(Pr^{2/3} - 1)} \left[1 + \left(\frac{d}{l}\right)^{2/3}\right] K \tag{24}$$

where

$$K = \begin{cases} \left(\frac{Pr_b}{Pr_w}\right)^{0.11} & \text{for liquids in the range } \frac{Pr_b}{Pr_w} = 0.05 - 20 \\ \left(\frac{T_c}{T_w}\right)^{0.45} & \text{for gases in the range } \frac{T_c}{T_w} = 0.5 - 1.5 \end{cases} \tag{25}$$

and T_c is the critical temperature. The friction factor, ξ, is calculated using the Filonenko correlation (Eq. (5)). Both Nu and ξ are evaluated using bulk properties. In the sCO_2 literature, Eq. (23) is far more often referenced as the famous 'Gnielinski correlation,' despite Eq. (24) being arguably more applicable to sCO_2 heat transfer due to the inclusion of correcting factors. Rarely do authors include both correlations in their discussion of Gnielinski's work. It is also worth noting that when Eq. (24) is referenced, the correcting factor K is often omitted without justification.

In 1977, Protopopov [43], using available experimental data, modified Eq. (12) from Krasnoshchekov and Protopopov [38] to apply to upward flow of sH_2O and sCO_2 in tubes under uniform heating. Protopopov [43] changed the exponent of the density correcting factor from 0.3 to 0.4 and added an additional correcting factor $\varphi(K)$. The modified local heat transfer correlation is given by the following

$$Nu = Nu_0 \left(\frac{\overline{c}_p}{c_{p,b}}\right)^n \left(\frac{\rho_w}{\rho_b}\right)^{0.4} \varphi(K) \tag{26}$$

where

$$K = \left[1 - \left(\frac{\rho_w}{\rho_b}\right)\right] Ri_b \tag{27}$$

Here, Nu_0 is the Petukhov and Kirillov correlation (Eq. (4)), which evaluates ξ using the Filonenko correlation (Eq. (5)). Both Nu_0 and ξ are evaluated using bulk properties. K, which encompasses the Richardson number Ri (defined in the Nomenclature), is representative of the buoyancy effects of natural convection on the local heat transfer. For $0.01 \leq K \leq 0.4$, $\varphi(K)$ is provided in Table 3. For $K \geq 0.4$, $\varphi(K) = 1.4K^{0.37}$.

Unlike previous modifications of Eq. (12) where the exponent n was determined graphically by Fig. 2., Protopopov [43] formulated an expression for n as follows

Journal of Heat Transfer. Received April 07, 2022;
Accepted manuscript posted August 25, 2022. doi:10.1115/1.4055345

$$n = \begin{cases} 0.4 & \text{when } \frac{\bar{c}_p}{c_{p,b}} < 1, \frac{T_w}{T_{pc}} < 1\text{, and } \frac{T_b}{T_{pc}} \geq 1.2 \\ n_1 = 0.22 + 0.18\frac{T_w}{T_{pc}} & \text{when } \frac{\bar{c}_p}{c_{p,b}} < 1 \text{ and } 1 \leq \frac{T_w}{T_{pc}} < 2.5 \\ n_1 - (5n_1 - 2)\left(\frac{T_b}{T_{pc}} - 1\right) & \text{when } \frac{\bar{c}_p}{c_{p,b}} < 1 \text{ and } 1 \leq \frac{T_b}{T_{pc}} < 1.2 \\ 0.7 & \text{when } \frac{\bar{c}_p}{c_{p,b}} > 1 \end{cases} \tag{28}$$

In the sCO_2 literature, the origins of Eq. (28) and its relation to n in Eq. (12) are debated. Equation (28) is often incorrectly cited as the same n used in Eq. (12) by Krasnoshchekov and Protopopov [38], despite there being no indication of a direct expression for n in that paper (only a graph). Upon careful inspection of [43], one finds that Protopopov acknowledges the differences between Eq. (12), derived for horizontal flow of uniformly heated sCO_2, and Eq. (26), derived for upward flow of uniformly heated sCO_2 and sH_2O. They also make a clear distinction between the n used in Eq. (12), which they provided plainly as $n = f(T_w/T_{pc}, T_b/T_{pc})$, and the n used in Eq. (26), which they gave as Eq. (28). It should then be apparent that Eq. (28) is not representative of the exponent n from Eq. (12), and should not be referenced as such. Protopopov likely left it as n to demonstrate the similar structure of their correlation to that of Krasnoshchekov and Protopopov [38].

In 1977, Baskov et al. [44] performed a set of experiments on upward flow of sCO_2 in a tube, cooled by a water-alcohol mixture, and developed the following local heat transfer correlation

$$Nu = Nu_0 \left(\frac{\bar{c}_p}{c_{p,w}}\right)^m \left(\frac{\rho_b}{\rho_w}\right)^n \tag{29}$$

where Nu_0 is the Petukhov and Kirillov correlation (Eq. (4)), which evaluates ξ using the Filonenko correlation (Eq. (5)). Both Nu_0 and ξ are evaluated using bulk properties. For $T_b/T_{pc} \leq 1$, $m = 1.4$ and $n = 0.15$. For $T_b/T_{pc} > 1$, m and n are provided in Table 4.

In 1979, Jackson and Hall [29] reviewed existing heat transfer correlations and modified Eq. (12) from Krasnoshchekov and Protopopov [38] such that the Nu_0 component, the Petukhov and Kirillov correlation (Eq. (4)), was replaced by a simpler Dittus-Boelter form (i.e., $Nu = C\, Re^m\, Pr^n$) as follows

$$Nu = 0.0183\, Re_b^{0.82}\, Pr_b^{0.5} \left(\frac{\rho_w}{\rho_b}\right)^{0.3} \left(\frac{\bar{c}_p}{c_{p,b}}\right)^n \tag{30}$$

where n is defined as

Journal of Heat Transfer. Received April 07, 2022;
Accepted manuscript posted August 25, 2022. doi:10.1115/1.4055345

$$n = \begin{cases} 0.4 & \text{for } T_b < T_w < T_{pc}\,, \text{ and } 1.2\,T_{pc} < T_b < T_w \\ 0.4 + 0.2\left(\frac{T_w}{T_{pc}} - 1\right) & \text{for } T_b < T_{pc} < T_w \\ 0.4 + 0.2\left(\frac{T_w}{T_{pc}} - 1\right)\left(1 - 5\left(\frac{T_b}{T_{pc}} - 1\right)\right) & \text{for } T_{pc} < T_b < 1.2\,T_{pc}\,, \text{ and } T_b < T_w \end{cases} \tag{31}$$

Similar to Eq. (28) from Protopopov [43], discussed earlier, the origins of Eq. (31) and its relation to n in Eq. (12) are debated in the sCO_2 literature. In fact, it is often the case that Eq. (28) and Eq. (31) are used interchangeably to define the n in Eq. (12), even with clear discrepancies between those two expressions and despite the absence of a direct expression for n in Krasnoshchekov and Protopopov [38] in the first place. Unlike Protopopov [43], however, Jackson and Hall [29] explicitly defined Eq. (31) as being the expression for n in both Eq. (30) and in Eq. (12). It then seems reasonable to assume that Jacskson and Hall [29] actually derived Eq. (31) exclusively from the work of Krasnoshchekov and Protopopov [38] and that Eq. (31) is an acceptable expression for n in Eq. (12). Since Krasnoshchekov and Protopopov [38] themselves did not formulate an expression for n, though, it is probably more appropriate to credit Eq. (31) to Jackson and Hall [29].

In the same work, Jackson and Hall [29] simplified Eq. (30) to the following

$$Nu = 0.0183\, Re_b^{0.82}\, \overline{Pr}_b^{0.5} \left(\frac{\rho_w}{\rho_b}\right)^{0.3} \tag{32}$$

where the specific heat correcting factor from Eq. (30) (which employed a mean value of 0.5 for n in this case) was combined with $Pr_b^{0.5}$ to form $\overline{Pr}_b^{0.5}$. The ranges of applicability for Eq. (30) and Eq. (32) were not provided by Jackson and Hall [29].

Also in 1979, Jackson and Hall [45] developed the following semi-empirical buoyancy parameter for supercritical fluids in heated vertical flows

$$Bu = \frac{\overline{Gr}_b}{Re_b^{2.7}} \tag{33}$$

This parameter is utilized in several subsequent sCO_2 heat transfer correlation studies to account for buoyancy effects in the flow, so it is worth formally defining here. Using this buoyancy parameter, Jackson and Hall [45] derived a local heat transfer correlation for supercritcal pressure CO_2 in heated downward flow

$$Nu = Nu_0\left(1 + 2750\, Bu^{0.91}\right)^{1/3} \tag{34}$$

However, the method for calculating Nu_0 was not specified in the paper, but it is likely defined the

Journal of Heat Transfer. Received April 07, 2022;
Accepted manuscript posted August 25, 2022. doi:10.1115/1.4055345

same as the Petukhov and Kirillov correlation (Eq. (4)).

In 1982, Watts and Chou [46] modified Jackson and Hall's correlation (Eq. (32)) to predict mixed convection heat transfer of sH_2O in heated vertical tubes by adding a buoyancy correcting function $f(Bu)$. Watts and Chou [46] also modified Jackson and Hall's buoyancy parameter (Eq. (33)) by including the Prandtl number. The modified local heat transfer correlation is given as

$$Nu = 0.021\, Re_b^{0.8}\, \overline{Pr}_b^{0.55} \left(\frac{\rho_w}{\rho_b}\right)^{0.35} f(Bu) \tag{35}$$

and the modified buoyancy parameter is

$$Bu = \frac{\overline{Gr}_b}{Re_b^{2.7}\, \overline{Pr}_b^{0.5}} \tag{36}$$

For upward flow, normal heat transfer

$$f(Bu) = \begin{cases} (1 - 3,000\, Bu)^{0.295} & \text{for } Bu < 10^{-4} \\ (7,000\, Bu)^{0.295} & \text{for } Bu \geq 10^{-4} \end{cases} \tag{37}$$

For upward flow, deteriorated heat transfer

$$f(Bu) = \begin{cases} (1.27 - 19,500\, Bu)^{0.7} & \text{for } Bu < 4.5 \cdot 10^{-5} \\ (2,600\, Bu)^{0.305} & \text{for } Bu \geq 4.5 \cdot 10^{-5} \end{cases} \tag{38}$$

For downward flow

$$f(Bu) = (1 + 30,000\, Bu)^{0.295} \tag{39}$$

Although this correlation and buoyancy parameter were originally developed for sH_2O, they were derived directly from work regarding sCO_2 and have influenced a number of subsequent sCO_2 heat transfer correlations, so they are worth including here.

Petrov and Popov [47], in 1985, simulated horizontal and vertical flow of sCO_2 in a tube under cooling conditions and developed the following local heat transfer correlation

$$Nu = Nu_0 \left(1 - m\,\frac{q}{G}\right) \left(\frac{\bar{c}_p}{c_{p,w}}\right)^n \tag{40}$$

where

$$n = \begin{cases} 0.66 - k\left(\frac{q}{G}\right) & \text{if } \bar{c}_p / c_{p,w} \leq 1 \\ 0.9 - k\left(\frac{q}{G}\right) & \text{if } \bar{c}_p / c_{p,w} > 1 \end{cases} \tag{41}$$

Here, Nu_0 is the Petukhov and Kirillov correlation (Eq. (4)), which evaluates ξ using the Filonenko

Journal of Heat Transfer. Received April 07, 2022;
Accepted manuscript posted August 25, 2022. doi:10.1115/1.4055345

correlation (Eq. (5)). Both Nu_0 and ξ are evaluated using wall properties. Here, $m = 0.001$ kg/J and $k = 4.10 \cdot 10^{-4}$ kg/J. The authors noted that although the introduction of the dimensional parameter q/G makes Eq. (40) suitable only for sCO_2, the simplicity of the resulting formula justified its introduction. The cofactor $1 - m(q/G)$ accounts for the fact that even at $\bar{c}_p/c_{p,w} = 1$, there are still physical property variations in the flow that affect local heat transfer.

In 1986, Ghajar and Asadi [48] compared existing near-critical heat transfer correlations and concluded that turbulent forced convective heat transfer to near-critical water and CO_2 could be sufficiently predicted by Dittus-Boelter-type correlations with the addition of correction factors to account for large local physical property variations. Ghajar and Asadi [48] then developed the following local heat transfer correlation for near-critical horizontal flow of CO_2 in tubes under heating conditions

$$Nu = 0.025\, Re_b^{0.8}\, Pr_b^{0.417} \left(\frac{\rho_w}{\rho_b}\right)^{0.32} \left(\frac{\bar{c}_p}{c_{p,b}}\right)^{n} \tag{42}$$

where n is determined using Eq. (31).

In 1988, Petrov and Popov [49] obtained the following generalized local heat transfer correlation for sH_2O, sCO_2, and supercritical Helium (sHe) in tubes under cooling conditions

$$Nu = \frac{(\xi/8)\, Re\, \overline{Pr}}{1.07 + 12.7\sqrt{\xi/8}\left[\overline{Pr}^{2/3}\sqrt{\frac{\rho_w}{\rho_b}}\left(1 - k_1\sqrt{\frac{|\xi_{ac}|}{\xi}}\right) - \left(1 - k_2\sqrt{\frac{|\xi_{ac}|}{\xi}}\right)\right]} \tag{43}$$

where, for sCO_2, $k_1 = 0.9$ and $k_2 = 1.0$. Petrov and Popov [49] derived the friction factor ξ as

$$\xi = \xi_0 \left(\frac{\mu_w}{\mu_b}\right)^{1/4} + 0.17\left(\frac{\rho_w}{\rho_b}\right)^{1/3} |\xi_{ac}| \tag{44}$$

where ξ_0 is calculated using the Filonenko correlation (Eq. (5)). $\xi_{ac} = -8q^+$ is an inertial factor to account for flow acceleration and was developed by Petrov and Popov in their previous work [47], and q^+ is a non-dimensional wall heat flux (defined in the Nomenclature). Both Nu and ξ are evaluated using bulk properties.

4 1990s - 2000s

There was a seemingly large gap in the development of sCO_2 heat transfer correlations between the late 1980s and 1990s. However, at the turn of the century, interest in correlating sCO_2 heat transfer data was revitalized due to potential applications of sCO_2 as an environmentally benign refrigerant in modern refrigeration, heat pump, and air conditioning cycles [50]. For each

Journal of Heat Transfer. Received April 07, 2022;
Accepted manuscript posted August 25, 2022. doi:10.1115/1.4055345

correlation presented in this section, information on type of boundary condition(s), flow direction(s), and operating conditions is found in Table 8.

In 1999, Fang [51] performed an extensive review of existing heat transfer and friction factor correlations for gas coolers. Based on Gnielinski's correlation (Eq. (23)) and Petrov and Popov's correlation (Eq. (40)), Fang obtained the following local heat transfer correlation for horizontal flow of sCO_2 in tubes under cooling conditions

$$Nu = \frac{(\xi/8)\,(Re - 1000)\,Pr}{A + 12.7\,\sqrt{\xi/8}\,(Pr^{2/3} - 1)} \left(1 - m\,\frac{q}{G}\right) \left(\frac{\bar{c}_p}{c_{p,w}}\right)^n \tag{45}$$

where

$$A = \begin{cases} 1 + 7 \cdot 10^{-8} Re_w & \text{if } Re_w < 1 \cdot 10^{-6} \\ 1.07 & \text{if } Re_w \geq 1 \cdot 10^{-6} \end{cases} \tag{46}$$

and the friction factor ξ is calculated as

$$\xi = \begin{cases} \frac{0.316}{Re^{1/4}} & \text{for } Re \leq 10^5 \\ (1.82\,log_{10}(Re)\ - 1.64)^{-2} & \text{for } 10^4 \leq Re \leq 5 \cdot 10^6 \end{cases} \tag{47}$$

Here, the first and second terms in the piece-wise function of ξ are, respectively, the Blasius and Filonenko friction factor correlations. Both Nu and ξ are evaluated using wall properties. The exponent n is calculated using Eq. (41), developed by Petrov and Popov [47]. The cofactor $1 - m(q/G)$ is the same as in Eq. (40), also developed by Petrov and Popov [47].

In 2002, Pitla et al. [52] experimentally and numerically investigated sCO_2 in a connected series of horizontal tube-in-tube counterflow heat exchangers, cooled by water in the annuli. Using their experimental and numerical results, Pitla et al. [52] then developed the following *mean* heat transfer correlation

$$Nu = \left(\frac{Nu_w + Nu_b}{2}\right) \frac{k_w}{k_b} \tag{48}$$

where Nu_w and Nu_b are evaluated using

$$Nu = \frac{(\xi/8)\,(Re - 1000)\,Pr}{1.07 + 12.7\,\sqrt{\xi/8}\,(Pr^{2/3} - 1)} \tag{49}$$

using exclusively wall and bulk properties, respectively. The friction factor, ξ, is calculated using the Filonenko correlation (Eq. (5)), and is evaluated using wall properties for Nu_w and bulk prop-

Journal of Heat Transfer. Received April 07, 2022;
Accepted manuscript posted August 25, 2022. doi:10.1115/1.4055345

330 erties for Nu_b. It should be noted that the *mean* heat transfer correlation is referring to the fact that
331 the wall and bulk Nusselt numbers are simply averaged together, and is not a reference to how the
332 properties are obtained in each. In fact, Pitla et al. [52] did not explicitly specify how the wall and
333 bulk properties were evaluated in Eqs. (48) and (49), i.e., averaged for each subsection, averaged
334 for the entire test section, or simply local values.

335 Pitla et al. [52] also referenced Eq. (49) as the Gnielinski correlation (Eq. (23)), but comparing
336 Eq. (49) to Eq. (23), it is clear that the first terms in the denominators do not match. The first term
337 in the denominator of Eq. (49) actually matches that of the Petukhov and Kirillov correlation
338 (Eq. (4)). For sake of clarity, it is still important here to provide exactly what was presented by
339 Pitla et al. [52].

340 In 2002, Liao and Zhao [53] performed experiments on sCO_2 in horizontal tubes of various
341 diameters under cooling conditions. The tubes were cooled using surrounding water passages.
342 Using their experimental data, Liao and Zhao [53] developed the following average heat transfer
343 correlation, based on average wall and bulk temperatures in the test section

$$\frac{Nu}{Nu_{db}} = 5.57 Ri_b^{0.205} \left(\frac{\rho_b}{\rho_w}\right)^{0.437} \left(\frac{\bar{c}_p}{c_{p,w}}\right)^{0.411} \tag{50}$$

344 where

$$Nu_{db} = 0.023\, Re^{0.8}\, Pr^{0.3} \tag{51}$$

345 is the Dittus-Boelter correlation for cooling, as introduced by McAdams [30, 54–56], and is eval-
346 uated using wall properties. The methods used to calculate average wall and bulk temperatures in
347 the test section are discussed in the original paper [53].

348 Liao and Zhao [57] also experimentally investigated horizontal, upward, and downward flow
349 of sCO_2 in tubes under heating conditions. The authors claimed the heat addition to the outer
350 copper tube wall enhanced lateral conduction in the test section, causing the boundary condition
351 to more closely resemble that of a constant wall temperature than a constant wall heat flux. Using
352 this constant wall temperature assumption in their analysis, Liao and Zhao [57] developed the
353 following local heat transfer correlations

354 For horizontal flow

$$Nu = 0.124\, Re_b^{0.8}\, Pr_b^{0.4} Ri_b^{0.203} \left(\frac{\rho_w}{\rho_b}\right)^{0.842} \left(\frac{\bar{c}_p}{c_{p,b}}\right)^{0.384} \tag{52}$$

355 For upward flow

$$Nu = 0.354\, Re_b^{0.8}\, Pr_b^{0.4}\, Bu^{0.157} \left(\frac{\rho_w}{\rho_b}\right)^{1.297} \left(\frac{\bar{c}_p}{c_{p,b}}\right)^{0.296} \tag{53}$$

Journal of Heat Transfer. Received April 07, 2022;
Accepted manuscript posted August 25, 2022. doi:10.1115/1.4055345

For downward flow

$$Nu = 0.643\, Re_b^{0.8}\, Pr_b^{0.4}\, Bu^{0.186} \left(\frac{\rho_w}{\rho_b}\right)^{2.154} \left(\frac{\overline{c}_p}{c_{p,b}}\right)^{0.751} \tag{54}$$

where Bu is the buoyancy parameter defined by Eq. (33) from Jackson and Hall [45].

Here, the buoyancy effects on the heat transfer in horizontal and vertical (upward and downward) flows are accounted for by the inclusion of parameters Ri_b and Bu, respectively. Interestingly, Liao and Zhao [57] were the first to formulate sCO_2 data into three separate equations based on flow orientation.

Similar to Pitla et al. [52], Yoon et al. [58] in 2003 experimented with sCO_2 in a connected series of horizontal tube-in-tube counterflow heat exchangers, cooled by water in the annuli. Yoon et al. [58] then modified Eq. (29) from Baskov et al. [44] to obtain the following average heat transfer correlation, based on average wall and bulk temperature in each subsection

$$Nu = 1.38\, Nu_0 \left(\frac{\overline{c}_p}{c_{p,w}}\right)^{0.86} \left(\frac{\rho_w}{\rho_b}\right)^{0.57} \tag{55}$$

In this equation, Nu_0 was not explicitly specified by Yoon et al. [58], but is likely calculated the same way as in Baskov et al. [44], using the Petukhov and Kirillov correlation (Eq. (4)), with ξ being evaluated using the Filonenko correlation (Eq. (5)). Yoon et al. [58] did specify, however, that Nu_0 is evaluated using wall properties. The methods used to obtain the average wall and bulk temperatures in each subsection are described in the original paper [58].

Acknowledging the difficulty of evaluating several physical properties at the wall in practice, Yoon et al. [58] simplified Eq. (55) to the following Dittus-Boelter form

$$Nu = \begin{cases} 0.14\, Re_b^{0.69}\, Pr_b^{0.66} & \text{for } T_b > T_{pc} \\ 0.013\, Re_b\, Pr_b^{-0.05} \left(\frac{\rho_{pc}}{\rho_b}\right)^{1.6} & \text{for } T_b \leq T_{pc} \end{cases} \tag{56}$$

The correlation was intentionally separated into regions of applicability above and below the pseudocritical temperature. Note that in the case of $T_b \leq T_{pc}$, which includes the region between the pseudocritical and critical temperature, a density-correcting factor was implemented to reflect the high variation in physical properties near those temperatures. Yoon et al. [58] deemed the inclusion of correcting factors unnecessary for $T_b > T_{pc}$.

In 2004, Dang and Hihara [18] experimentally investigated sCO_2 in a horizontal tube-in-tube counterflow heat exchanger, cooled by water in the annulus. Dang and Hihara [18] then proposed the following average heat transfer correlation, based on average wall, bulk, and film temperatures in the test section, as a modification to the Gnielinski correlation (Eq. (23))

Journal of Heat Transfer. Received April 07, 2022;
Accepted manuscript posted August 25, 2022. doi:10.1115/1.4055345

$$Nu = \frac{(\xi_f/8)\,(Re_b - 1000)\,Pr}{1.07 + 12.7\,\sqrt{\xi_f/8}\,(Pr^{2/3} - 1)} \tag{57}$$

where

$$Pr = \begin{cases} \frac{c_{p,b}\,\mu_b}{k_b} & \text{for } c_{p,b} \geq \bar{c}_p \\ \frac{\bar{c}_p\,\mu_b}{k_b} & \text{for } c_{p,b} < \bar{c}_p \text{ and } \frac{\mu_b}{k_b} \geq \frac{\mu_f}{k_f} \\ \frac{\bar{c}_p\,\mu_f}{k_f} & \text{for } c_{p,b} < \bar{c}_p \text{ and } \frac{\mu_b}{k_b} < \frac{\mu_f}{k_f} \end{cases} \tag{58}$$

Here, the friction factor, ξ_f, is calculated using the Filonenko correlation (Eq. (5)) and is evaluated using film properties. The methods used to obtain average wall, bulk, and film temperatures in the test section are discussed in the original paper [18]. All physical properties were then appropriately evaluated using these average temperatures. Similar to Pitla et al. [52], Dang and Hihara [18] misrepresented the actual first term in the denominator of the Gnielinski correlation (Eq. (23)) by using 1.07 instead of 1.

It should be noted that no information was given about the water-side. For each case, Dang and Hihara [18] reported their wall heat flux as remaining constant along the length of the test section despite the inherent, and non-uniform, conjugate boundary condition present in their heat exchanger. This is especially true when the bulk sCO_2 temperature approaches the pseudocritical temperature, where the local heat transfer and physical properties are subject to high variations under small temperature changes. Additionally, as described by Chao et al. [59], non-uniformity in the wall heat flux may also be caused by lateral conduction in the copper tube used by Dang and Hihara [18], again in regions where the bulk sCO_2 temperature approaches the pseudocritical temperature.

In 2006, Son and Park [60] experimentally investigated sCO_2 in a connected series of horizontal tube-in-tube counterflow heat exchangers, cooled by water in the annuli. Son and Park [60] then developed the following local heat transfer correlation, based on average wall and bulk temperatures computed in each sub-section

$$Nu = \begin{cases} Re_b^{0.55}\,Pr_b^{0.23}\left(\frac{c_{p,b}}{c_{p,w}}\right)^{0.15} & \text{for } T_b > T_{pc} \\ Re_b^{0.35}\,Pr_b^{1.9}\left(\frac{\rho_b}{\rho_w}\right)^{-1.6}\left(\frac{c_{p,b}}{c_{p,w}}\right)^{-3.4} & \text{for } T_b \leq T_{pc} \end{cases} \tag{59}$$

The methods used to obtain average wall and bulk temperatures in each subsection are discussed in the original paper [60]. All physical properties were then appropriately evaluated using these average temperatures. Similar to Eq. (56) from Yoon et al. [58], Eq. (59) was intentionally

Journal of Heat Transfer. Received April 07, 2022;
Accepted manuscript posted August 25, 2022. doi:10.1115/1.4055345

separated into regions of applicability above and below the pseudocritical temperature. Again in the case of $T_b \leq T_{pc}$, which includes the region between the pseudocritical and critical temperature, a density correcting factor was implemented to reflect the high variation in physical properties near those temperatures. Unlike Yoon et al. [58], however, Son and Park [60] found it necessary to include a specific heat correcting factor in both cases.

In 2007, Huai and Koyama [61] performed experiments on sCO_2 in a horizontal multi-port test section consisting of 10 circular channels that were cooled by water flowing inside copper blocks surrounding the channels. Huai and Koyama [61] then developed the following average heat transfer correlation, based on average wall and bulk temperatures in a single channel

$$Nu = 0.0222\, Re_b^{0.8}\, Pr_b^{0.3} \left(\frac{\rho_b}{\rho_w}\right)^{-1.47} \left(\frac{\bar{c}_p}{c_{p,w}}\right)^{0.083} \tag{60}$$

The methods used to obtain average wall and bulk temperatures are discussed in the original paper [61]. All physical properties were then appropriately evaluated using these average temperatures.

In 2007, Kim et al. [62] performed experiments on vertical flow of sCO_2 in circular, triangular, and square channels under uniform heating and developed the following local heat transfer correlation

$$Nu = Nu_F \left(\frac{\xi_M}{\xi_F}\right) \left(\frac{\bar{c}_p}{c_{p,b}}\right)^{0.6} \left(\frac{\rho_w}{\rho_b}\right)^{n} \tag{61}$$

where

$$Nu_F = 0.0243\, Re^{0.8}\, Pr^{0.4} \tag{62}$$

is the non-dimensionalized form of the original Dittus-Boelter correlation for heating [54,55], and is evaluated using bulk properties. The friction factor for mixed convection, ξ_M, is defined as

$$\xi_M = \frac{8\tau_w}{\rho_b \mu_b^2} \tag{63}$$

and the friction factor for forced convection, ξ_F, is defined as

$$\xi_F = \frac{1}{(1.8\, log_{10}(Re_b) - 1.5)^2} \tag{64}$$

Here, the forced convection friction factor (Eq. (64)) is very similar to the Filonenko correlation (Eq. (5)). However, Kim et al. [62] did not claim Eq. (64) to be the Filonenko correlation (Eq. (5)), so perhaps it is appropriate to credit it to Kim et al. [62] with influence from Filonenko [28]. The

Journal of Heat Transfer. Received April 07, 2022;
Accepted manuscript posted August 25, 2022. doi:10.1115/1.4055345

exponent n is a correction index to account for varying channel geometry, and is defined as

$$n = 0.955 - 0.0087 \left(\frac{q}{G}\right) + 1.30 \cdot 10^{-5} \left(\frac{q}{G}\right)^2 \tag{65}$$

Kuang et al. [63], in 2008, correlated their experimental data for sCO_2 in a horizontal multi-port test section with 11 circular channels, cooled by water, using Eq. (23) from Gnielinski [32], Eq. (12) from Krasnoshchekov and Protopopov [38], Eq. (42) from Ghajar and Asadi [48], Eq. (48) from Pitla et al. [52], and Eq. (60) from Huai et al. [61]. Kuang et al. [63] then developed the following average heat transfer correlation, based on average wall and bulk temperatures in the test section, to more accurately predict their data

$$Nu = 0.001546\, Re_b^{1.054}\, Pr_b^{0.653} \left(\frac{\rho_w}{\rho_b}\right)^{0.367} \left(\frac{\bar{c}_p}{c_{p,b}}\right)^{0.4} \tag{66}$$

The methods used to obtain average wall and bulk temperatures in the test section were not discussed in the original paper [63].

In 2008, Kim et al. [64] experimentally investigated upward flow of supercritical pressure CO_2 in a tube under uniform heating and modified the constants in Eq. (32) from Jackson and Hall [29] to more accurately correlate their data. The modified local heat transfer correlation is as follows

$$Nu = 0.0182\, Re_b^{0.824}\, \overline{Pr}_b^{0.515} \left(\frac{\rho_w}{\rho_b}\right)^{0.299} \tag{67}$$

In 2009, Bae and Kim [65], following their previous work [64], performed additional experiments regarding upward flow of supercritical pressure CO_2 in tubes and an annular channel under uniform heating. This time, however, Bae and Kim [65] modified Eq. (30) from Jackson and Hall [29] by replacing the leading coefficient 0.0183 with 0.021, the leading coefficient of Eq. (35) from Watts and Chou [46], and adding their own buoyancy correcting function $f(Bu)$, similar to what was done by Watts and Chou [46]. The modified local heat transfer correlation is as follows

$$Nu = 0.021\, Re_b^{0.82}\, Pr_b^{0.5} \left(\frac{\rho_w}{\rho_b}\right)^{0.3} \left(\frac{\bar{c}_p}{c_{p,b}}\right)^{n} f(Bu) \tag{68}$$

where

Journal of Heat Transfer. Received April 07, 2022;
Accepted manuscript posted August 25, 2022. doi:10.1115/1.4055345

$$f(Bu) = \begin{cases} (1 + 10^8\, Bu)^{-0.032} & \text{for } 5 \cdot 10^{-8} < Bu < 7 \cdot 10^{-7} \\ 0.0185\, Bu^{-0.43465} & \text{for } 7 \cdot 10^{-7} < Bu < 10^{-6} \\ 0.75 & \text{for } 10^{-6} < Bu < 10^{-5} \\ 0.0119\, Bu^{-0.36} & \text{for } 10^{-5} < Bu < 3 \cdot 10^{-5} \\ 32.4\, Bu^{0.4} & \text{for } 3 \cdot 10^{-5} < Bu < 10^{-4} \end{cases} \tag{69}$$

and n is determined using Eq. (31).

In 2009, Bruch et al. [66] experimentally investigated sCO_2 in a vertical tube-in-tube counter-flow heat exchanger, cooled by water in the annulus. Bruch et al. [66] then modified Eq. (32) from Jackson and Hall [29] by incorporating a buoyancy parameter Bu, given by Eq. (33) from Jackson and Hall [45], and by separating the correlation into separate flow regimes to better predict the entire dataset. The resulting correlations, especially Eq. (71), take a similar form to that of Eq. (34) from Jackson and Hall [45]. The set of average heat transfer correlations, based on average wall and bulk temperatures in the test section, are as follows

For turbulent-aiding mixed convection

$$Nu = \begin{cases} Nu_{FC}\,(1 - 75\, Bu^{0.46}) & \text{for } Bu < 4.2 \cdot 10^{-5} \\ Nu_{FC}\,(13.5\, Bu^{0.40}) & \text{for } Bu > 4.2 \cdot 10^{-5} \end{cases} \tag{70}$$

For turbulent-opposing mixed convection

$$Nu = Nu_{FC}\left(1.542 + 3243\, Bu^{0.91}\right)^{1/3} \tag{71}$$

Here, Nu_{FC} is given by Eq. (32) from Jackson and Hall [29], and Bu is the buoyancy parameter defined by Eq. (33) from Jackson and Hall [45]. The methods used to obtain average wall and bulk temperatures are discussed in the original paper [66]. All physical properties were then appropriately evaluated using these average temperatures.

5 2010s - Present (Modern Developments)

For each correlation presented in this section, information on type of boundary condition(s), flow direction(s), and operating conditions is found in Table 9. In 2010 Bae et al. [67], following their previous works [64, 65], performed additional experiments on upward and downward flow of sCO_2 in a tube under uniform heating. Although they did not explicitly state this, it is clear by inspection that Bae et al. [67] implemented Eq. (68) from their previous study [65] with modifications to the Re exponent and the buoyancy correcting function $f(Bu)$. The former was changed from 0.82 to 0.8 (a very subtle difference), but the latter was formulated into three separate flow

Journal of Heat Transfer. Received April 07, 2022;
Accepted manuscript posted August 25, 2022. doi:10.1115/1.4055345

regimes to better predict the heat transfer throughout the entire experimental dataset. The new local heat transfer correlation is as follows

$$Nu = 0.021\, Re_b^{0.8}\, Pr_b^{0.5} \left(\frac{\rho_w}{\rho_b}\right)^{0.3} \left(\frac{\bar{c}_p}{c_{p,b}}\right)^{n} f(Bu) \tag{72}$$

For upward flow, normal heat transfer

$$f(Bu) = \begin{cases} (1 + 3 \cdot 10^5\, Bu)^{0.35} & \text{for } Bu < 2 \cdot 10^{-6} \\ 0.48\, Bu^{-0.07} & \text{for } Bu > 2 \cdot 10^{-6} \end{cases} \tag{73}$$

For upward flow, deteriorated heat transfer

$$f(Bu) = \begin{cases} 1 & \text{for } Bu < 2 \cdot 10^{-7} \\ 0.043\, Bu^{-0.2} & \text{for } 2 \cdot 10^{-7} < Bu < 6 \cdot 10^{-6} \\ 1120\, Bu^{0.64} & \text{for } 6 \cdot 10^{-6} < Bu < 1.5 \cdot 10^{-5} \\ 3.6 \cdot 10^{-8}\, Bu^{-1.53} & \text{for } 1.5 \cdot 10^{-5} < Bu < 4 \cdot 10^{-5} \\ 200\, Bu^{0.68} & \text{for } 4 \cdot 10^{-5} < Bu < 2 \cdot 10^{-4} \end{cases} \tag{74}$$

For downward flow

$$f(Bu) = \begin{cases} 1 & \text{for } Bu < 10^{-7} \\ 0.153\, Bu^{-0.117} & \text{for } 10^{-7} < Bu < 8 \cdot 10^{-6} \\ 15.8\, Bu^{0.28} & \text{for } 8 \cdot 10^{-6} < Bu < 5 \cdot 10^{-5} \end{cases} \tag{75}$$

Here, n is determined using Eq. (31).

In the same year, Li et al. [68] experimentally investigated upward and downward flow of sCO_2 in tubes under uniform heating and developed the following local heat transfer correlation

$$\frac{Nu}{Nu_f} = \begin{cases} \left[1 + Bu^{0.1} \left(\frac{\bar{c}_p}{c_{p,b}}\right)^{-0.3} \left(\frac{\rho_w}{\rho_b}\right)^{0.5} \left(\frac{Nu}{Nu_f}\right)^{-2}\right]^{0.46} & \text{for downward flow} \\ \left[\left|1 - Bu^{0.1} \left(\frac{\bar{c}_p}{c_{p,b}}\right)^{-0.009} \left(\frac{\rho_w}{\rho_b}\right)^{0.35} \left(\frac{Nu}{Nu_f}\right)^{-2}\right|\right]^{0.46} & \text{for upward flow} \end{cases} \tag{76}$$

where Bu is a buoyancy parameter defined as

$$Bu = \frac{Gr_{q,b}}{Re_b^{3.425}\, Pr_b^{0.8}} \tag{77}$$

and Nu_f is calculated using Eq. (30) from Jackson and Hall [29] multiplied by a correction factor ϵ_l, defined as

Journal of Heat Transfer. Received April 07, 2022;
Accepted manuscript posted August 25, 2022. doi:10.1115/1.4055345

$$\epsilon_l = 1 + 2.35\, Pr_b^{-0.4}\, Re_b^{-0.15} \left(\frac{x}{d}\right)^{-0.6} exp\left(-0.39\, Re_b^{0.1} \left(\frac{x}{d}\right)\right) \tag{78}$$

The exponent n in Nu_f (Eq. (30)) is determined using Eq. (31).

Still in 2010, Oh and Son [69], following their previous work [60], again experimentally investigated sCO_2 in a connected series of horizontal tube-in-tube counterflow heat exchangers, cooled by water in the annuli. Oh and Son [69] then developed the following local heat transfer correlation, based on average wall and bulk temperatures computed in each sub-section

$$Nu = \begin{cases} 0.023\, Re_b^{0.7}\, Pr_b^{2.5} \left(\frac{c_{p,b}}{c_{p,w}}\right)^{-3.5} & \text{for } T_b/T_{pc} > 1 \\ 0.023\, Re_b^{0.6}\, Pr_b^{3.2} \left(\frac{\rho_b}{\rho_w}\right)^{3.7} \left(\frac{c_{p,b}}{c_{p,w}}\right)^{-4.6} & \text{for } T_b/T_{pc} \leq 1 \end{cases} \tag{79}$$

The methods used to obtain average wall and bulk temperatures in each subsection are discussed in the original paper [69]. All physical properties were then appropriately evaluated using these average temperatures. Similar to Eqs. (56) and (59) from Yoon et al. [58] and Son and Park [60], respectively, Eq. (79) was intentionally separated into regions of applicability above and below the pseudocritical temperature. In the case of $T_b \leq T_{pc}$, which includes the region between the pseudocritical and critical temperature, a density correcting factor was implemented to reflect the high variation in physical properties near those temperatures. Similar to Son and Park [60], Oh and Son [69] also found it necessary to include a specific heat correcting factor in both cases.

In 2010, Kim and Kim [70] experimentally investigated upward flow of sCO_2 in tubes under uniform heating. They determined that Eq. (12) from Krasnoshchekov and Protopopov [38] predicted their experimental data adequately when buoyancy and flow acceleration effects were negligible, but failed to do so when these effects grew stronger. Kim and Kim [70] then developed the following local heat transfer correlation to more accurately predict their data and account for the aforementioned flow effects

$$Nu = 0.226\, Re_b^{1.174}\, Pr_b^{1.057} \left(\frac{\rho_w}{\rho_b}\right)^{0.571} \left(\frac{\bar{c}_p}{c_{p,b}}\right)^{1.032} Ac^{0.489}\, Bu^{0.0021} \tag{80}$$

where Ac is a flow acceleration parameter defined as

$$Ac = \frac{q_b^+}{Re_b^{0.625}} \left(\frac{\mu_w}{\mu_b}\right) \left(\frac{\rho_b}{\rho_w}\right)^{0.5} \tag{81}$$

and Bu is a buoyancy parameter defined as

Journal of Heat Transfer. Received April 07, 2022;
Accepted manuscript posted August 25, 2022. doi:10.1115/1.4055345

$$Bu = \frac{Gr_{q,b}}{Re_b^{3.425}\, Pr_b^{0.8}} \left(\frac{\mu_w}{\mu_b}\right) \left(\frac{\rho_b}{\rho_w}\right)^{0.5} \tag{82}$$

Here, q^+ is the non-dimensional wall heat flux (defined in the Nomenclature) and is evaluated using bulk properties. Also, Gr_q is the Grashof number based on wall heat flux (defined in the Nomenclature) and is evaluated using bulk properties. Interestingly, Kim and Kim. [70] were the first to implement property correcting factors directly into their buoyancy and flow acceleration parameters, an idea which first appeared in the sCO_2 heat transfer correlation literature in 1979 by Jackson and Hall [29].

In 2011 Kim and Kim [71], following their previous work [70], performed an additional experiment for downward flow of sCO_2 in tubes under uniform heating. Using the data from both experiments, Kim and Kim [71] developed the following local heat transfer correlation for upward and downward flow of sCO_2

$$Nu = 2.0514\, Re_b^{0.928}\, Pr_b^{0.742} \left(\frac{\rho_w}{\rho_b}\right)^{1.305} \left(\frac{\mu_w}{\mu_b}\right)^{-0.669} \left(\frac{\bar{c}_p}{c_{p,b}}\right)^{0.888} \left(q_b^+\right)^{0.792} \tag{83}$$

In 2011 Kim and Kim [72], using the experimental data presented in their previous work [70], also developed a two-layer heat transfer model for upward flow of sH_2O and sCO_2 in tubes under uniform heating. The model is based on thermal resistance behavior in both the viscous sub-layer and buffer layer, and accounts for significant flow acceleration and specific heat variations. The local heat transfer correlation for sCO_2 is given as

$$\begin{aligned} \frac{1}{Nu} &= \frac{1}{Nu_{VSL}} + \frac{1}{Nu_{BFL}} \\ &= \frac{0.00249\, \mu_b}{d\, \sqrt{\rho_b\, \tau_{w,iso}}} \left(\frac{\rho_w}{\rho_b}\right)^{-3.461} \left(\frac{\mu_w}{\mu_b}\right)^{3.357} Re_b^{-0.412} \left(q^+\right)^{-1.621} + \frac{1}{0.192\, Re_b^{0.625}\, Pr_b^{0.597}\, \left(\bar{c}_p/c_{p,b}\right)^{0.826}} \end{aligned} \tag{84}$$

Here, $1/Nu_{VSL}$ and $1/Nu_{BFL}$ are the thermal resistances in the viscous sub-layer and buffer layer, respectively. $\tau_{w,iso}$ is the wall shear stress due to flow acceleration, evaluated at isothermal fluid properties.

In 2011 Bae [73], expanding on their previous works [64, 65, 67], performed addititional experiments on upward and downward flow of sCO_2 in both a tube and an annular channel under uniform heating. Using the heat transfer correlation from Watts and Chou [46] (Eq. (35)), the buoyancy parameter from Jackson and Hall [45] (Eq. (33)), and a new buoyancy correcting function $f(Bu)$, Bae [73] developed the following local heat transfer correlation

Journal of Heat Transfer. Received April 07, 2022;
Accepted manuscript posted August 25, 2022. doi:10.1115/1.4055345

$$Nu = 0.021\, Re_b^{0.8}\, \overline{Pr}_b^{0.55} \left(\frac{\rho_w}{\rho_b}\right)^{0.35} f(Bu) \tag{85}$$

where for tubes

$$f(Bu) = \begin{cases} (1 - 8,000\, Bu)^{0.5} & \text{for upward flow and } Bu < 10^{-4} \\ 15\, Bu^{0.38} & \text{for upward flow and } Bu > 10^{-4} \\ (1 + 30,000\, Bu)^{0.3} & \text{for downward flow and all } Bu \end{cases} \tag{86}$$

and for annular channels

$$f(Bu) = \begin{cases} (1 - 10,000\, Bu)^{1.5} & \text{for upward flow and } Bu < 5 \cdot 10^{-5} \\ (1 - 5,000\, Bu)^{1.5} & \text{for downward flow and } Bu < 5 \cdot 10^{-5} \end{cases} \tag{87}$$

Here, Bu is the buoyancy parameter defined by Eq. (33) from Jackson and Hall [45]. Similar to $f(Bu)$ from Bae et al. [67], $f(Bu)$ here was formulated into separate flow regimes and geometries to better predict the heat transfer throughout the entire experimental dataset.

In 2011, Fang and Xu [16] reviewed existing heat transfer correlations for sCO_2 in tubes under cooling conditions. Fang and Xu [16] then used Eq. (45) from Fang [51] as a reference for developing the following local heat transfer correlation

$$Nu = \frac{(\xi/8)\,(Re_b - 20\, Re_b^{0.5})\, \overline{Pr}_b}{1 + 12.7\sqrt{\xi/8}\,(\overline{Pr}_b^{2/3} - 1)} \left(1 + 0.001\, \frac{q}{G}\right) \tag{88}$$

where ξ is a modified friction factor, defined as

$$\xi = \xi_{noniso} - 1.36 \left(\frac{\mu_w}{\mu_b}\right)^{-1.92} \xi_{ac} \tag{89}$$

where ξ_{ac} is an acceleration friction factor, defined as

$$\xi_{ac} = \frac{d}{l}\,(\rho_{b,out} + \rho_{b,in}) \left(\frac{1}{\rho_{b,out}} - \frac{1}{\rho_{b,in}}\right) \tag{90}$$

and ξ_{noniso} is a nonisothermal single-phase friction factor, defined as

$$\xi_{noniso} = \xi_{iso,b} \left(\frac{\mu_w}{\mu_b}\right)^{0.49(\rho_f/\rho_{pc})^{1.31}} \tag{91}$$

where ξ_{iso} is an isothermal single-phase friction factor, defined as

Journal of Heat Transfer. Received April 07, 2022;
Accepted manuscript posted August 25, 2022. doi:10.1115/1.4055345

$$\xi_{iso} = 1.613 \left[ln \left(0.234 \left(\frac{\epsilon}{d} \right)^{1.1007} - \frac{60.525}{Re_b^{1.1105}} + \frac{56.291}{Re_b^{1.0712}} \right) \right]^{-2} \quad (92)$$

Here, ϵ is the tube wall roughness.

Mokry and Pioro [74] experimentally investigated upward flow of sCO_2 in a tube under uniform heating, in 2011, and developed the following local heat transfer correlation

$$Nu = 0.0121\, Re_b^{0.86}\, \overline{Pr}_b^{0.23} \left(\frac{\rho_w}{\rho_b} \right)^{0.59} \quad (93)$$

In 2012 Preda et al. [75], using available data from the literature, developed the following local heat transfer correlation for horizontal and vertical flow of sCO_2 in tubes

$$Nu = 0.0015\, Re_w^{1.03}\, \overline{Pr}_w^{0.76} \left(\frac{\rho_w}{\rho_b} \right)^{0.46} \left(\frac{\mu_w}{\mu_b} \right)^{0.53} \left(\frac{k_w}{k_b} \right)^{-0.43} \quad (94)$$

One year later, Gupta et al. [25], using available experimental data from the literature, developed a set of local heat transfer correlations for upward flow of sCO_2 in tubes under uniform heating. Each of the correlations utilizes a different reference temperature to evaluate Re and Pr to determine which approach best predicts the experimental data for use in subsequent studies. The resulting set of local heat transfer correlations is as follows

Bulk-temperature approach

$$Nu = 0.01\, Re_b^{0.89}\, \overline{Pr}_b^{-0.14} \left(\frac{\rho_w}{\rho_b} \right)^{0.93} \left(\frac{k_w}{k_b} \right)^{0.22} \left(\frac{\mu_w}{\mu_b} \right)^{-1.13} \quad (95)$$

Film-temperature approach

$$Nu = 0.0043\, Re_f^{0.94} \left(\frac{\rho_w}{\rho_b} \right)^{0.57} \left(\frac{k_w}{k_b} \right)^{-0.52} \quad (96)$$

Wall-temperature approach

$$Nu = 0.0038\, Re_w^{0.96}\, \overline{Pr}_w^{-0.14} \left(\frac{\rho_w}{\rho_b} \right)^{0.84} \left(\frac{k_w}{k_b} \right)^{-0.75} \left(\frac{\mu_w}{\mu_b} \right)^{-0.22} \quad (97)$$

Gupta et al. [25] stated their preliminary analysis indicated that Eq. (97), the wall-temperature approach, predicts the reference dataset most accurately.

Also in 2013, Saltanov et al. [26] performed a similar analysis to their previous study [25] by using available experimental data from the literature to develop a set of local heat transfer correlations for upward flow of sCO_2 in tubes under uniform heating. Like before, each correlation utilizes a different reference temperature to evaluate Re and Pr. This time, however, a correlation utilizing the film-temperature approach was omitted. The resulting set of local heat transfer

Journal of Heat Transfer. Received April 07, 2022;
Accepted manuscript posted August 25, 2022. doi:10.1115/1.4055345

correlations is as follows

Bulk-temperature approach

$$Nu = 0.0035\, Re_b^{0.97}\, \overline{Pr}_b^{0.71} \left(\frac{\rho_w}{\rho_b}\right)^{0.42} \left(\frac{\mu_w}{\mu_b}\right)^{0.33} \tag{98}$$

Wall-temperature approach

$$Nu = 0.0047\, Re_w^{0.94}\, \overline{\overline{Pr}}^{0.7} \left(\frac{\rho_w}{\rho_b}\right)^{-0.16} \left(\frac{\mu_w}{\mu_b}\right)^{0.94} \tag{99}$$

Here, $\overline{\overline{Pr}}$ is the integrated Prandtl number, defined in the Nomenclature. It is important here to differentiate between $\overline{\overline{Pr}}$ and $\overline{Pr}$. By definition, the former uses an integral approach for evaluating all properties within the Prandtl number (i.e. μ, c_p, and k), whereas the latter only uses an integral approach for evaluating c_p within the Prandtl number. Also note that $\overline{Pr}$ appears far more often than $\overline{\overline{Pr}}$ in the sCO_2 literature. Similar to their previous study [25], Saltanov et al. [26] again concluded that the wall-temperature approach predicts the reference dataset most accurately.

In 2014, Liu et al. [76] performed experiments on sCO_2 in a horizontal tube-in-tube counter-flow heat exchanger, cooled by water in the annulus. Liu et al. [76] then developed the following heat transfer correlation, based on average wall and bulk temperatures in the test section

$$Nu = 0.01\, Re_w^{0.9}\, Pr_w^{0.5} \left(\frac{\rho_w}{\rho_b}\right)^{0.906} \left(\frac{c_{p,w}}{c_{p,b}}\right)^{-0.585} \tag{100}$$

The methods used to obtain average wall and bulk temperatures in the test section are discussed in the original paper [76]. All physical properties were then appropriately evaluated using these average temperatures.

In 2015, Saltanov et al. [77], following their previous works [25, 26], revised an experimental sCO_2 dataset (by removing certain data points) from the available literature and reconstructed their previous local heat transfer correlations to the following for upward flow of sCO_2 in tubes under uniform heating in the normal heat transfer regime

$$Nu = 0.0164\, Re_b^{0.823}\, \overline{Pr}_b^{0.195} \left(\frac{\rho_w}{\rho_b}\right)^{0.374} \tag{101}$$

In the same work, Saltanov et al. [77] developed the following preliminary local heat transfer correlation for upward flow of sCO_2 in tubes under uniform heating in the normal heat transfer regime, based on a combination of two revised experimental sCO_2 datasets

$$Nu = 0.0331\, Re_b^{0.784}\, \overline{Pr}_b^{0.444} \left(\frac{\rho_w}{\rho_b}\right)^{0.64} \tag{102}$$

Journal of Heat Transfer. Received April 07, 2022;
Accepted manuscript posted August 25, 2022. doi:10.1115/1.4055345

Saltanov et al. [77], based on the same revised experimental dataset used to develop Eq. (101), also developed the following correlation for upward flow of sCO_2 in tubes under uniform heating in the deteriorated heat transfer regime

$$Nu = 9.3886\, Nu_0^{0.9467} \left(\frac{P}{P_c}\right)^{-0.5196} \left(\frac{T_b}{T_{pc}}\right)^{2.5939} \left(\frac{10^4 q}{G \cdot h_b}\right)^{-0.2858} \left(\frac{\mu_b}{\mu_w}\right)^{0.2244} \left(\frac{k_b}{k_w}\right)^{-0.4083} \left(\frac{\overline{c}_p}{c_{p,b}}\right)^{0.764} \quad (103)$$

where Nu_0 is evaluated using

$$Nu_0 = \frac{(\xi/8)\, Re\, \overline{Pr}}{1.07 + 12.7\sqrt{\xi/8}\,(\overline{Pr}^{2/3} - 1)} \quad (104)$$

and the friction factor, ξ, is calculated using the Filonenko correlation (Eq. (5)). Both Nu_0 and ξ are evaluated using bulk properties. h_b is the specific enthalpy, evaluated using bulk properties. Note Eq. (104) is very similar to the Petukhov and Kirillov correlation (Eq. (4)). As mentioned previously, a common misconception in the current literature is the use of $\overline{Pr}$ instead of Pr in the numerator of Eq. (4), as is the case here. Regardless, it is still important here to reiterate exactly what was presented by Saltanov et al. [77].

Saltanov [78], in 2015, following their previous works [25, 26, 77] and using available experimental data from the literature, developed a correlation for upward flow of sCO_2 in tubes under uniform heating in the normal heat transfer regime. This time, however, the bulk-temperature approach was deemed most suitable. The resulting local heat transfer correlation is as follows

$$Nu = 0.0052\, Re_b^{0.937}\, \overline{Pr}_b^{-0.242} \left(\frac{\rho_w}{\rho_b}\right)^{0.854} \left(\frac{\mu_w}{\mu_b}\right)^{-1.37} \left(\frac{k_w}{k_b}\right)^{0.426} \quad (105)$$

In 2016, Ma et al. [79] experimentally investigated sCO_2 in a tube-in-tube counterflow heat exchanger, cooled by water in the annulus. The heat exchanger flow orientation (horizontal or vertical) was not explicitly specified. Similar to Bruch et al. [66], Ma et al. [79] modified Eq. (32) from Jackson and Hall [29] to incorporate the buoyancy parameter Bu from Eq. (33) by Jackson and Hall [45]. Unlike Bruch et al. [66], however, Ma et al. [79] correlated their data using a single expression. The resulting average heat transfer correlation, based on average wall and bulk temperatures in the test section, is as follows

$$Nu = Nu_{FC}\left(2.61 - 86.965\, Bu^{0.458}\right) \quad (106)$$

Here, Nu_{FC} is given by Eq. (32) from Jackson and Hall [29], and Bu is the buoyancy parameter defined by Eq. (33) from Jackson and Hall [45]. The methods used to obtain average wall and bulk

Journal of Heat Transfer. Received April 07, 2022;
Accepted manuscript posted August 25, 2022. doi:10.1115/1.4055345

temperatures in the test section are discussed in the original paper [79].

In 2016, Yang [80] performed a numerical investigation on horizontal flow of supercritical pressure CO_2 in a tube under uniform cooling conditions and developed the following local heat transfer correlation based on their simulation data

$$Nu = 1.39\, Re_b^{0.72}\, Pr^{0.52} \left(\frac{\rho_w}{\rho_b}\right)^{0.288} \left(\frac{\overline{c}_p}{c_{p,b}}\right)^{0.44} \tag{107}$$

Note that Yang [80] did not specify at which temperature (wall, bulk, or film) Pr was evaluated.

Also in 2016, Liu et al. [81] experimentally investigated vertical flow of sCO_2 in a tube under uniform heating and developed the following local heat transfer correlation

$$Nu = 0.022\, Re_b^{1.03}\, \overline{Pr}_b^{0.58} \left(\frac{\rho_w}{\rho_b}\right)^{0.57} Bu^{0.026} \tag{108}$$

where Bu is the buoyancy parameter defined by Eq. (33) from Jackson and Hall [45].

In 2017 Liu et al. [82], following their previous work [81], experimentally investigated upward and downward flows of sCO_2 in tubes under heating conditions to further examine buoyancy and flow acceleration effects. Liu et al. [82] then developed the following local heat transfer correlation

$$Nu = 0.00075\, Re_b^{0.93}\, \overline{Pr}_b^{0.68} \left(\frac{\rho_w}{\rho_b}\right)^{0.42} exp\left(Bu^{-0.023}\right)\, exp\left(Ac^{0.079}\right) \left[1 + \frac{2.63}{l/d}\right] \tag{109}$$

where Ac is a flow acceleration parameter defined as

$$Ac = \frac{4\, q^+\, \beta_b\, T_b}{d} \frac{d}{Re_b^{0.625}} \left(\frac{\mu_w}{\mu_b}\right) \left(\frac{\rho_b}{\rho_w}\right)^{0.5} \tag{110}$$

and Bu is a buoyancy parameter defined as

$$Bu = \frac{\overline{Gr}_b}{Pr_w^{0.4}\, Re_b^{2.625}} \left(\frac{\rho_b}{\rho_w}\right)^{0.5} \left(\frac{\mu_w}{\mu_b}\right) \tag{111}$$

Here, β is the volume expansion coefficient, defined in the Nomenclature, and is evaluated using bulk properties. Note that the acceleration and buoyancy parameters here are very similar to Eqs. (81) and (82), respectively, developed by Kim and Kim [70], and were directly compared to one another by Liu et al. [82].

In 2018, Zhang et al. [83] performed experiments on sCO_2 in a horizontal tube-in-tube counterflow heat exchanger, cooled by water in the annulus. Zhang et al. [83] also performed supplemental numerical simulations of horizontal flow of sCO_2 in a tube under a constant heat flux cool-

Journal of Heat Transfer. Received April 07, 2022;
Accepted manuscript posted August 25, 2022. doi:10.1115/1.4055345

ing boundary condition. Using the experimental and numerical data separately, Zhang et al. [83] developed the following local heat transfer correlations

Using the experimental data

$$Nu = 0.138\, Re_b^{0.68}\, Pr_b^{0.07} \left(\frac{\rho_b}{\rho_w}\right)^{-0.74} \left(\frac{\bar{c}_p}{c_{p,b}}\right)^{-0.31} Ri_b^{0.08} \left[1 + \left(\frac{d}{l}\right)^{2/3}\right] \tag{112}$$

Using the numerical data

$$Nu = 0.000567\, Re_b^{1.23}\, Pr_b^{0.83} \left(\frac{\rho_b}{\rho_w}\right)^{0.86} \left(\frac{\bar{c}_p}{c_{p,b}}\right)^{0.76} Ri_b^{0.16} \left[1 + \left(\frac{d}{l}\right)^{2/3}\right] \tag{113}$$

It should be noted that the geometry correcting factor $\left[1 + (d/l)^{2/3}\right]$ is exactly that of the Gnielinski correlation (Eq. (24)). However, Zhang et al. [83] failed to mention the origin or derivation of this term in the context of their study, nor did they give credit to Gnielsinki [32]. Additionally, Zhang et al. [83] intentionally applied a constant wall heat flux (cooling) boundary condition in the simulations to simplify the inherent conjugate boundary condition in their heat exchanger from the experiment. As alluded to in the discussion of Dang and Hihara's work [18] and in Chao et al. [84], it is important to realize that a constant heat flux boundary condition (or constant wall temperature for that matter) may not adequately represent a conjugate boundary condition in terms of local heat transfer phenomena.

In 2018, Zhang et al. [85] experimentally investigated upward flow of sCO_2 in a tube under uniform heating. The experiments were conducted at intentionally low mass fluxes to evaluate the heat transfer enhancement induced by dominating buoyancy effects. Zhang et al. [85] then developed the following local heat transfer correlation

$$Nu = \begin{cases} 0.00672\, Re_b^{1.414}\, \overline{Pr}_b^{-0.005} \left(\frac{\rho_w}{\rho_b}\right)^{0.448} \left(\frac{\bar{c}_p}{c_{p,b}}\right)^{0.218} Bu^{0.586} & \text{if } h_b < 0.9\, h_{pc} \\ 0.059\, Re_b^{0.829}\, \overline{Pr}_b^{0.35} \left(\frac{\rho_w}{\rho_b}\right)^{-0.095} \left(\frac{\bar{c}_p}{c_{p,b}}\right)^{0.214} Bu^{0.142} & \text{if } h_b \geq 0.9\, h_{pc} \end{cases} \tag{114}$$

Here, Bu is the buoyancy parameter defined by Eq. (33) from Jackson and Hall [45]. Zhang et al. [85] noted that due to the sharpest variations of physical properties being at the pseudocritical temperature, dividing the correlation directly at the pseudocritical point would likely result in non-continuous predictions. From their data, Zhang et al. [85] instead determined that dividing their correlation at $h_b/h_{pc} = 0.9$ would suffice.

In 2018, Fan and Tang [86] simulated upward flow of sCO_2 in a tube under non-uniform heating. Fan and Tang [86] then modified an sH_2O correlation developed by Mokry et al. [74] to obtain the following local heat transfer correlation for sCO_2

Journal of Heat Transfer. Received April 07, 2022;
Accepted manuscript posted August 25, 2022. doi:10.1115/1.4055345

$$Nu = 0.0061\, Re_b^{0.904}\, \overline{Pr}_b^{0.684} \left(\frac{\rho_w}{\rho_b}\right)^{0.564} \left(\frac{\mu_w}{\mu_b}\right)^{-0.184} \tag{115}$$

In 2019, Fan et al. [21] performed an extensive review of existing heat transfer correlations for sCO_2 in tubes under uniform heating. Fan et al. [21] then modified Eq. (115) from their previous work [86] by implementing specific heat, axial flow acceleration, and non-uniform heat flux correction factors to obtain the following

$$Nu = 0.0061\, Re_b^{0.904}\, \overline{Pr}_b^{0.684} \left(\frac{\rho_w}{\rho_b}\right)^{0.564} \left(\frac{\mu_w}{\mu_b}\right)^{-0.184} \left(\frac{\bar{c}_p}{c_{p,b}}\right)^{0.679} \left(q^+\right)^{-0.0598} \left(\frac{q_{avg}}{q_{max}}\right)^{-0.709} \tag{116}$$

where q_{avg} and q_{max} are the average and maximum heat fluxes on the wall, respectively.

In the same year, Kim et al. [87] experimentally investigated horizontal flow of sCO_2 in a tube under uniform heating to observe buoyancy and flow acceleration effects on heat transfer to the top and bottom tube walls. Kim et al. [87] then derived the following local heat transfer model, with separate natural and forced convection components, for supercritical pressure CO_2

$$Nu = \sqrt{Nu_{fc}^2 + Nu_{nc}^2} \tag{117}$$

where Nu_{fc} is the forced convection component given as

$$Nu_{fc} = c_1\, Re_b^{0.8}\, Pr_b^{0.4} \frac{Q_b^{n_3}}{Re_b^{n_1}\, Pr_b^{n_2}} \left(\frac{\bar{\rho}}{\rho_b}\right)^{n_4} \left(\frac{\bar{\mu}}{\mu_b}\right)^{n_5} \left(\frac{\bar{k}}{k_b}\right)^{n_6} \tag{118}$$

and Nu_{nc} is the natural convection component given as

$$\frac{1}{Nu_{nc}} = c_2\, Gr_{q,b}^{m_1}\, Pr_b^{m_2} \left(\frac{\bar{\rho}}{\rho_b}\right)^{m_3} \left(\frac{\bar{\mu}}{\mu_b}\right)^{m_4} \left(\frac{\bar{c}_p}{c_{p,b}}\right)^{m_5} \left(\frac{\bar{k}}{k_b}\right)^{m_6} \tag{119}$$

Here the constants $c_1 - c_2$, $n_1 - n_6$, $m_1 - m_6$ are provided in Table 5, and are defined for both the top and bottom of the tube wall. Kim et al. [87] define Q_b as the fluid expansion due to thermal loading and is given as

$$Q_b = \frac{\beta_b\, q\, d}{k_b} \tag{120}$$

In 2019, Wang et al. [88] numerically studied horizontal flow of sCO_2 in tubes under uniform cooling and obtained the following average heat transfer correlation, based on average wall, bulk, and film temperatures in the test section

Journal of Heat Transfer. Received April 07, 2022;
Accepted manuscript posted August 25, 2022. doi:10.1115/1.4055345

$$Nu = 1.2838\, Nu_0 \left(\frac{\rho_w}{\rho_b}\right)^{-0.1458} \tag{121}$$

where, similar to Eq. (57) by Dang and Hihara [18], Nu_0 here is a modification of the Gnielsinski correlation (Eq. (23)), given as

$$Nu_0 = \frac{(\xi_f/8)\,(Re_b - 1000)\,\overline{Pr}_f}{1.07 + 12.7\sqrt{\xi_f/8}\,(\overline{Pr}_f^{2/3} - 1)} \tag{122}$$

Here, the friction factor, ξ_f, is calculated using the Filonenko correlation (Eq. (5)) and is evaluated using film properties. The methods used to obtain average wall, bulk, and film temperatures in the test section are discussed in the original paper [89].

In 2019, Zhang et al. [89] experimentally investigated upward and downward flow of sCO_2 in a tube under uniform heating and varying mass fluxes to examine buoyancy and flow acceleration effects on heat transfer. Using a combination of their data and several other experimental datasets from the available literature, Zhang et al. [89] developed the following local heat transfer correlation

$$\frac{Nu}{Nu_{DB}} = \left[\left|1 \pm \frac{2300\,Gr}{Re^{2.625}\,Pr^{0.4}}\left(\frac{\mu_w}{\mu_b}\right)^{0.56}\left(\frac{Nu}{Nu_{DB}}\right)^{0.5} - \frac{10^4\,q^+}{Re^{0.625}}\left(\frac{\mu_w}{\mu_b}\right)^{0.56}\left(\frac{Nu}{Nu_{DB}}\right)^{0.5}\right|\right]^{0.53}\left(\frac{\rho_w}{\rho_b}\right)^{0.3}\left(\frac{\overline{c}_p}{c_{p,b}}\right)^{n} \tag{123}$$

where

$$n = \begin{cases} 0.41 & \text{if } \frac{\alpha}{\alpha_{DB}} > 0.3 \\ 0.55 & \text{if } \frac{\alpha}{\alpha_{DB}} < 0.3 \text{ or } \frac{\alpha}{\alpha_{DB}} > 1 \end{cases} \tag{124}$$

and

$$Nu_{DB} = 0.023\, Re^{0.8}\, Pr^{0.4} \tag{125}$$

is the Dittus-Boelter correlation for heating, as introduced by McAdams [30, 54–56]. α_{DB} is the heat transfer coefficient calculated from Nu_{DB}. Regarding the plus-minus sign in Eq. (123), the positive sign applies for downward flow and the negative sign applies for upward flow. It should be noted that Zhang et al. [89] did not specify at which temperature (wall, bulk, or film) Gr, Re, and Pr were evaluated.

Journal of Heat Transfer. Received April 07, 2022;
Accepted manuscript posted August 25, 2022. doi:10.1115/1.4055345

In 2020 Zhang et al. [90], following their prior work [89], experimentally and numerically investigated sCO_2 in vertical and horizontal tubes under heating conditions. Zhang et al. [90] validated Eq. (123) for sCO_2 in vertical flows from their previous work [89], and established the following heat transfer correlations for sCO_2 in horizontal tubes with buoyancy.

The average heat transfer is given by

$$Nu_{avg} = 0.00514\, Re^{0.94}\, Pr^{0.69} \left(1 + 0.0197 \left(\frac{\overline{Gr}_q}{Gr_{th}}\right)^{-2.91}\right) \left(\frac{\bar{c}_p}{c_{p,b}}\right)^{0.70} \left(\frac{\rho_w}{\rho_b}\right)^{0.67} \tag{126}$$

The average heat transfer on the lower surface is given by

$$\frac{Nu_{lower}}{Nu_{avg}} = \left(\frac{\bar{c}_p}{c_{p,b}}\right)^{0.02} \left(\frac{\rho_w}{\rho_b}\right)^{0.28} \left(1 + 1.54 \left(\frac{\overline{Gr}_q}{Gr_{th}}\right)\right)^{0.08} \tag{127}$$

The average heat transfer on the upper surface is given by

$$\frac{Nu_{lower}}{Nu_{upper}} = \left(\frac{\bar{c}_p}{c_{p,b}}\right)^{0.02} \left(\frac{\rho_w}{\rho_b}\right)^{0.23} \left(1 + 1.2 \left(\frac{\overline{Gr}_q}{Gr_{th}}\right)\right)^{0.08} \tag{128}$$

Here, Nu_{avg} is the average heat transfer in the test section, Nu_{lower} is the average heat transfer on the lower tube surface, and Nu_{upper} is the average heat transfer on the upper tube surface. $(\overline{Gr}_q/Gr_{th})$ is a buoyancy parameter originally proposed by Polyakov [91] in 1974. $\overline{Gr}_q$ is defined in the Nomenclature and Gr_{th} is defined as

$$Gr_{th} = \sqrt{Pr}\, Re^{2.75} \left(\frac{1 + 2.4\left(Pr^{2/3} - 1\right)}{Re^{1/8}}\right) \tag{129}$$

It is important to note that Zhang et al. [90] did not specify the methods of obtaining their reference wall and bulk temperatures. Zhang et al. [90] also did not specify at which temperature (wall, bulk, or film) $\overline{Gr}_q$, Gr_{th}, Re, and Pr were evaluated.

Also in 2020, Guo et al. [92] experimentally investigated horizontal flow of sCO_2 in a tube under uniform heating and high q/G conditions. Using their experimental data, Guo et al. [92] compared existing correlations and determined they could not adequately predict heat transfer under high q/G conditions. Guo et al. [92] then proposed the following average heat transfer correlation, based on average wall and bulk temperatures in the test section

$$Nu = 0.114\, Re_b^{0.589}\, \overline{Pr}_b^{0.465}\, Ri_b^{-0.125} \left(\frac{\rho_w}{\rho_b}\right)^{0.240} \left(\frac{\bar{c}_p}{c_{p,b}}\right)^{0.096} \tag{130}$$

The methods used to obtain average wall and bulk temperatures in the test section are discussed in the original paper [92].

Journal of Heat Transfer. Received April 07, 2022;
Accepted manuscript posted August 25, 2022. doi:10.1115/1.4055345

Liu et al. [93] experimentally and numerically investigated upward flow of sCO_2 in a tube under uniform heating in 2020. Liu et al. [93] then modified Eq. (30) from Jackson and Hall [29] to better predict heat transfer in the $T_b < T_{pc}$ regime as follows

$$Nu = \begin{cases} 0.0183\, Re_b^{0.82}\, Pr_b^{0.5} \left(\frac{\rho_w}{\rho_b}\right)^{0.3} \left(\frac{\bar{c}_p}{c_{p,b}}\right)^{n} & \text{if } T_b \geq T_{pc} \\ \frac{d}{k}\left(\frac{1}{\alpha_{jackson}} + \frac{\delta_{Bo}}{k_r}\right)^{-1} & \text{if } T_b < T_{pc} \end{cases} \tag{131}$$

where n is determined using Eq. (31), $\alpha_{jackson}$ is the heat transfer coefficient calculated using Nu obtained by Eq. (30) from Jackson and Hall [29], δ_{Bo} is the re-laminarization thickness as discussed in [93], and k_r is the thermal conductivity evaluated at $0.5(T_w + T_{pc})$. Note here that for $T_b \geq T_{pc}$, Eq. (131) is identical to Eq. (30) from Jackson and Hall [29]. The numerical simulations implemented a 2D axisymmetric model.

In the same year, Zhu et al. [94] also experimentally investigated upward flow of sCO_2 in tubes under uniform heating, in addition to assessing the effects of pseudoboiling on supercritical heat transfer. Using their data and other experimental datasets from the available literature (including data for CO_2, water, and R134a), Zhu et al. [94] then developed the following local heat transfer correlation for sCO_2

$$Nu = 0.0012\, Re_b^{0.9484}\, \overline{Pr}_b^{0.718}\, K^{-0.0313} \tag{132}$$

where K is a new dimensionless parameter, given as

$$K = \left(\frac{q}{G\, h_w}\right)^2 \frac{\rho_b}{\rho_w} \tag{133}$$

and is representative of the evaporation-induced momentum force relative to the inertial force of the fluid. Zhu et al. [94] derived K to govern the growth of wall attached vapor-like fluid layer thickness, which, according to their assertion, dominates supercritical heat transfer.

In 2020, Wang et al. [95] experimentally investigated horizontal flow of sCO_2 in tubes under uniform heating. To account for heat flux and inlet temperature effects on local heat transfer, Wang et al. [95] introduced a non-dimensional temperature T^*. Wang et al. [95] then developed the following local heat transfer correlation

$$Nu = 0.225\, Re_b^{0.423}\, Pr_b^{0.229}\, Ri_b^{-0.156}\, (T^*)^{0.055} \left(\frac{\bar{c}_p}{c_{p,b}}\right)^{0.401} \tag{134}$$

where T^* is the non-dimensional temperature, given as

Journal of Heat Transfer. Received April 07, 2022;
Accepted manuscript posted August 25, 2022. doi:10.1115/1.4055345

$$T^* = \frac{T_{pc} - T_b}{T_{b,out} - T_{b,in}} \tag{135}$$

The next year, Wang et al. [96], following their previous work [95], experimentally investigated upward flow of sCO_2 in tubes under uniform heating. Again utilizing their non-dimensional temperature, T^*, Wang et al. [96] developed the following local heat transfer correlation

$$Nu = 0.0019\, Re_b^{0.997}\, Pr_b^{0.599}\, (T^*)^{0.03} \left(\frac{c_{p,w}}{c_{p,b}}\right)^{0.634} \left(\frac{k_w}{k_b}\right)^{0.192} \left(\frac{\mu_w}{\mu_b}\right)^{-0.333} \tag{136}$$

where T^* is defined by Eq. (135).

In 2021, Wahl et al. [97] experimentally investigated sCO_2 in a horizontal tube-in-tube parallel-flow heat exchanger, cooled by water in the annulus. Wahl et al. [97] then determined a wall-temperature approach best correlated their data, and formulated the following local heat transfer correlation

$$Nu = \begin{cases} 0.0495\, Re_w^{0.771}\, Pr_w^{0.455} \left(\frac{\rho_b}{\rho_w}\right)^{1.450} \left(\frac{\bar{c}_p}{c_{p,b}}\right)^{-0.026} \left(\frac{k_b}{k_w}\right)^{1.604} \left(\frac{\mu_b}{\mu_w}\right)^{-2.623} & \text{if } T_w \geq T_{pc} \\ 0.0052\, Re_w^{0.971}\, Pr_w^{0.388} \left(\frac{\rho_b}{\rho_w}\right)^{1.279} \left(\frac{\bar{c}_p}{c_{p,b}}\right)^{0.450} \left(\frac{k_b}{k_w}\right)^{2.158} \left(\frac{\mu_b}{\mu_w}\right)^{-2.923} & \text{if } T_w < T_{pc} \end{cases} \tag{137}$$

Like several other previously discussed investigations [58, 60, 69, 93], Wahl et al. [97] intentionally separated Eq. (137) into regions of applicability above and below the pseudocritical temperature.

Viswanathan and Krishnamoorthy [98], in 2021, numerically investigated horizontal laminar flow of sCO_2 in tubes under uniform heating conditions, and developed the following local heat transfer correlation

$$Nu = 4.36 \left(\frac{c_{p,w}}{c_{p,b}}\right)^{0.35} \left(\frac{\mu_w}{\mu_b}\right)^{2.38} \left(\frac{k_w}{k_b}\right)^{-2.06} \left(\frac{\rho_w}{\rho_b}\right)^{-0.9} \tag{138}$$

In 2021, Wang et al. [99] experimentally investigated horizontal flow of sCO_2 in tubes under uniform heating. Wang et al. [99] modified Eq. (30) from Jackson and Hall [29] by adding a thermal conductivity correcting factor, a buoyancy parameter (via the Richardson number), and a non-dimensional heat flux term as follows

$$Nu = 0.0183\, Re_b^{0.82}\, Pr_b^{0.5} \left(\frac{\rho_w}{\rho_b}\right)^{0.3} \left(\frac{\bar{c}_p}{c_{p,b}}\right)^{n} \left(\frac{k_w}{k_b}\right)^{0.04} exp\left(Ri_b^{2.3}\right)\, exp\left(\left(q_b^+\right)^{0.7}\right) \tag{139}$$

where n is determined by the following

Journal of Heat Transfer. Received April 07, 2022;
Accepted manuscript posted August 25, 2022. doi:10.1115/1.4055345

$$n = \begin{cases} 0.52 & \text{for } T_b < T_w < T_{pc}\text{, and } 1.2\,T_{pc} < T_b < T_w \\ 0.52 + 0.2\left(\frac{T_w}{T_{pc}} - 1\right) & \text{for } T_b < T_{pc} < T_w \\ 0.52 + 0.2\left(\frac{T_w}{T_{pc}} - 1\right)\left(1 - 5\left(\frac{T_b}{T_{pc}} - 1\right)\right) & \text{for } T_{pc} < T_b < 1.2\,T_{pc}\text{, and } T_b < T_w \end{cases} \tag{140}$$

Note that Eq. (140) is almost identical to Eq. (31) from Jackson and Hall [29], with the only difference being the leading term in each case was changed from 0.4 to 0.52.

6 Beyond Correlation-based Predictions

From the preceding review, it is evident that there have been numerous attempts at correlating the heat transfer behavior of sCO_2 in terms of Nusselt number. One may argue the reason for the large number of correlation development efforts is the poor accuracy near the pseudocritical line. The sharply varying properties cause instances of deteriorated or enhanced heat transfer, resulting from strong buoyancy and acceleration effects. The large property gradients with pressure and temperature contribute to large uncertainties, potentially multiple orders of magnitude [11]. The use of a computational fluid dynamics approach to predict the heat transfer coefficient depends on the turbulence model selected and is not cost effective in the long run. When utilizing computational results from the literature, supercritical fluids demand a clear articulation of the reference temperature utilized when results are averaged [100].

As a result, some researchers have turned to ML and ANN (also known as nueral networks (NN)) to predict heat transfer coefficients and wall temperatures for flows of sCO_2. The role of ML as a new paradigm for thermal science and engineering problems is an idea that gained footing in the 2000s [101] and has become increasingly popular as a new tool to obtain accurate predictions of heat transfer results [102–108]. It is important to note that with ML-based approaches, the traditional non-dimensional framework, i.e., $Nu = f(Re, Pr)$, is not necessarily needed. For sCO_2, this is advantageous because it reduces the number of material properties needed as an input to predict thermal behavior, thus alleviating uncertainties that will cause errors in the predicted heat transfer coefficient. Since non-dimensionalization is not needed, many ML algorithms in the literature report either the heat transfer coefficient or the wall temperature directly.

To obtain a ML model, first, a very large data set is obtained either from existing literature or developed in-house via experiments or computational fluid dynamics simulations. Part of the data is used for training and validating the ML algorithms, and then the heat transfer coefficients or wall temperatures are predicted for the remaining data and other points of interest. For each ML study presented in this section, information on the input(s), output(s), and operating range is presented

Journal of Heat Transfer. Received April 07, 2022;
Accepted manuscript posted August 25, 2022. doi:10.1115/1.4055345

in Table 10.

Work on using ANN to predict sCO_2 thermal behavior began as early as 2003. Scalabrin and Piazza [109] used the data of Olson and Allen [110] to develop four different correlation architectures to predict the thermal behavior of sCO_2 in a heated horizontal tube. Four different correlation architectures were considered to either predict the Nusselt number or the heat transfer coefficient directly as a function of either dimensionless groups and/or directly accessible physical quantities. The multilayer feedforward network (MFLN) with one hidden layer was implemented due to its effectiveness as an approximator of continuous functions in a compact space. The NN predictions were compared against the correlation that Olson and Allen [110] recommended as the best available at the time, which was essentially Eq. (12) with Nu_0 defined by Eq. (24), rather than defined by Eq. (4).

Scalabrin and Piazza [109] found that NN heat transfer models in the forms of 3.) and 4.) from Table 10 both appear to predict the data sets at least as accurately as the conventional equation recommended by Olson and Allen [110]. The investigators in [109] concluded that results presented in either dimensionless groups or physical variables was equally effective.

Using the same data [110], correlation architectures, and conventional correlation for comparison as Scalabrin and Piazza [109], Chen et al. [111], in 2005, investigated three different NN approaches: back-propogation neural network (BPN), radial basis function network (RBFN), and modified RBFN (MRBFN). They found that the MRBFN with 10 neurons performed better than the other NN methods and the conventional correlation due to its ability to predict large changes in the near-critical region. In 2010, Pesteei and Mehrabi [112] used experimental data extracted from [113] to predict the local heat transfer coefficient for low-Reynolds number sCO_2 flows. They used a group method of data handling (GMDH) type of ANN and found good predictive agreement with the experimental data. Unlike prior investigators, Pesteei and Mehrabi [112] did not test their GMDH method with conventional correlations.

Later, in 2018, Chu et al. [114] combined direct numerical simulation (DNS) with deep neural networks (DNN) to predict wall temperatures and wall shear stresses for sCO_2 heated in a horizontal tube. Five input parameters, diameter, inlet pressure, inlet temperature, bulk specific enthalpy, and heat flux, were used to determine two output parameters, wall temperature and wall shear stress. Chu et al. [114] also did not test their DNN with conventional correlations as the motive of their work was to show that a combination of DNS and DNN was able to reduce computational load and still provide the same accuracy as DNS alone.

In 2019, using literature compiled from a wide range of investigators ([67, 68, 70–72, 81, 115–123]) that captured heated sCO_2 flowing vertically upward, Ye et al. [124] developed ANN models to predict the wall temperature as a function of diameter, pressure, mass flux, bulk specific enthalpy,

Journal of Heat Transfer. Received April 07, 2022;
Accepted manuscript posted August 25, 2022. doi:10.1115/1.4055345

and heat flux. They assessed the ANN model against a wide variety of available correlations, including non-supercritical specific equations like the Dittus-Boelter correlation, as introduced by McAdams (Eq. (51)), and the best-performing correlations with respect to the ANN data, the Jackson and Hall correlation (Eq. (30)) and the Kim et al. correlation [125]. Note that the Kim et al. correlation [125] was actually developed for sCO_2 flow through a narrow annulus and not a tube geometry, thus not included in the review of correlations presented here.

In 2021, Zhu et al. [126] performed experiments for heated sCO_2 flowing upward in a vertical tube. They combined their data with five other independent investigators [68, 82, 85, 123, 127], encompassing a range of parameters and developed an ANN model to predict the wall temperature as a function of pressure, mass flux, heat flux, bulk specific enthalpy, and diameter. The ANN model was compared to Jackson and Hall (Eq. (30)), and three correlations developed for supercritical water [128–130], and it was found that the ANN model outperformed the correlations.

Sun et al. [131], in 2021, utilized a genetic algorithm - back propagation (GA-BP) NN to predict wall temperatures for vertical sCO_2 flows using the same input parameters as [124, 126]. They used data from several different investigators [67, 70–72, 81, 115, 116, 119–122], many that were the same as Ye et al. [124]. Like others, the GA-BP ANN method was compared against four traditional correlations, including Eqs. (1, 30, 94, 97). As others before, they found that ANN methods predicted heat transfer behavior the best. Follow-on work by Sun et al. [132], using the same experimental data sets as their prior work [131], describes the development of an ANN model for predicting the wall temperature and heat transfer coefficient for upward sCO_2 flow. They validated their model with the same conventional correlations as [131], with the addition of the Dittus-Boelter correlation, as introduced by McAdams (Eq. (51)). For the case of predicting the heat transfer coefficient, and subsequently the Nusselt number, the initial parameters were converted to physical, dimensionless parameters.

Very recently, Prasad et al. [133] used a commercial computational fluid dynamics software (ANSYS Fluent) to generate a data set required to train a NN algorithm to predict the Nusselt number for heated sCO_2 flowing vertically upward. A comparative study was performed to select the most effective turbulence model, which was found to be the k-epsilon RNG with enhanced wall treatment. Unlike many other investigators, Prasad et al. [133] did not compare their results with conventional correlations.

While it is evident that the application of ML is proving to be an efficient and accurate way to predict heat transfer coefficients, there is still a gap in research due the inaccessibility of the algorithms and modified networks used in the preceding literature. Furthermore, the data ML algorithms use to predict thermal behavior of sCO_2 are limited in the number of data points and scope. Nevertheless, the ability of ML algorithms to capture the highly non-linear behavior of heat

Journal of Heat Transfer. Received April 07, 2022;
Accepted manuscript posted August 25, 2022. doi:10.1115/1.4055345

transfer in supercritical fluids makes them an attractive alternative to traditional correlation-based prediction approaches.

7 Concluding Remarks

A comprehensive review and discussion of sCO_2 heat transfer correlations in straight, round tubes was presented from a historical perspective in this work. Starting with early investigations in the late 1950s through the present day, each correlation was introduced along with pertinent information regarding its development, utilization, and operating limitations. Heat transfer correlations have become progressively more complex with the inclusion of multiple correcting factors (accounting for sharp thermophysical property variations), integrated properties, individual terms that change with flow conditions, and buoyancy and flow acceleration parameters. Advancements in statistical techniques used to develop and modify these correlations, including multiple linear regression, as well as the inherent advancement in understanding the thermal and flow phenomena of sCO_2 are largely responsible for the increased complexity.

Additionally, several correlations presented here are simply modifications of other correlations, most often to correlate heat transfer data for a different set of operating or geometrical conditions. Despite both the growing sophistication of, and modifications to, sCO_2 heat transfer correlations, there has not been a substantial increase in predictive capabilities [20, 23]. Modern correlations are generally only applicable under relatively small ranges of operating conditions, in specific flow orientations, and using tubes of particular geometric features. This is due to the heightened sensitivity of physical properties (including thermal conductivity and specific heat) along the pseudocritical line and especially near the critical point. From an applications perspective it is advantageous to operate near these conditions to maximize heat transfer benefits, which is why the majority of experimental and numerical efforts have been focused there, but traditional predictive methods are consequently hindered. This explains why a consensus has not been, and likely will not be, reached on an accepted 'best' sCO_2 heat transfer correlation (using traditional correlation development techniques) whose applicability spans a wide array of operating, flow, and geometric specifications.

While ML and ANN techniques are nascent methods to replace conventional sCO_2 correlations, they have shown promise in more accurately predicting the thermal behavior of sCO_2 flows. However, the studies presented thus far are light on data and limited in scope.

Journal of Heat Transfer. Received April 07, 2022;
Accepted manuscript posted August 25, 2022. doi:10.1115/1.4055345

References

[1] Brunner, G., 2010, "Applications of supercritical fluids," Annual Review of Chemical and Biomolecular Engineering, **1**, pp. 321–342.

[2] Knez, Ž., Markočič, E., Leitgeb, M., Primožič, M., Hrnčič, M. K., and Škerget, M., 2014, "Industrial applications of supercritical fluids: A review," Energy, **77**, pp. 235–243.

[3] Qi, H., Gui, N., Yang, X., Tu, J., and Jiang, S., 2018, "The application of supercritical CO2 in nuclear engineering: A review," The Journal of Computational Multiphase Flows, **10**(4), pp. 149–158.

[4] Yang, C.-Y. and Liao, K.-C., 2017, "Effect of Experimental Method on the Heat Transfer Performance of Supercritical Carbon Dioxide in Microchannel," J of Heat Transfer-Transactions of the ASME, **139**(11).

[5] Guo, J. and Huai, X., 2017, "Performance Analysis of Printed Circuit Heat Exchanger for Supercritical Carbon Dioxide," J of Heat Transfer-Transactions of the ASME, **139**(6).

[6] Crespi, F., Gavagnin, G., Sánchez, D., and Martínez, G. S., 2017, "Supercritical carbon dioxide cycles for power generation: A review," Applied Energy, **195**, pp. 152–183.

[7] Liao, G., Liu, L., Jiaqiang, E., Zhang, F., Chen, J., Deng, Y., and Zhu, H., 2019, "Effects of technical progress on performance and application of supercritical carbon dioxide power cycle: A review," Energy Conversion and Management, **199**, p. 111986.

[8] Krishna, A. B., Jin, K., Ayyaswamy, P. S., Catton, I., and Fisher, T. S., 2022, "Modeling of Supercritical CO2 Shell-and-Tube Heat Exchangers Under Extreme Conditions. Part I: Correlation Development," J of Heat Transfer-Transactions of the ASME, **144**(5).

[9] Krishna, A. B., Jin, K., Ayyaswamy, P. S., Catton, I., and Fisher, T. S., 2022, "Modeling of Supercritical CO2 Shell-and-Tube Heat Exchangers Under Extreme Conditions: Part II: Heat Exchanger Model," J of Heat Transfer-Transactions of the ASME, **144**(5).

[10] Fronk, B. M. and Rattner, A. S., 2016, "High-Flux Thermal Management With Supercritical Fluids," J of Heat Transfer-Transactions of the ASME, **138**(12).

[11] Sullivan, N. P., Chao, Y., Boetcher, S. K. S., and Ricklick, M. A., 2021, "Impact of Uncertainty on Prediction of Supercritical CO2 Properties and Nusselt Numbers," J of Heat Transfer-Transactions of the ASME, **143**(10).

[12] Pitla, S., Robinson, D., Groll, E., and Ramadhyani, S., 1998, "Heat Transfer from Supercritical Carbon Dioxide in Tube Flow: A Critical Review," HVAC&R Research, **4**(3), pp. 281–301.

[13] Pioro, I. L., Khartabil, H. F., and Duffey, R. B., 2004, "Heat transfer to supercritical fluids flowing in channels—empirical correlations (survey)," Nuclear Engineering and Design, **230**(1-3), pp. 69–91.

[14] Duffey, R. B. and Pioro, I. L., 2005, "Experimental heat transfer of supercritical carbon dioxide flowing inside channels (survey)," Nuclear Engineering and Design, **235**(8), pp. 913–924.

[15] Cheng, L., Ribatski, G., and Thome, J. R., 2008, "Analysis of supercritical CO2 cooling in macro- and micro-channels," International Journal of Refrigeration, **31**(8), pp. 1301–1316.

[16] Fang, X. and Xu, Y., 2011, "Modified heat transfer equation for in-tube supercritical CO2 cooling," Applied Thermal Engineering, **31**(14-15), pp. 3036–3042.

[17] Lin, W., Du, Z., and Gu, A., 2011, "Analysis on heat transfer correlations of supercritical

CO2 cooled in horizontal circular tubes," Heat and Mass Transfer, **48**(4), pp. 705–711.

[18] Dang, C. and Hihara, E., 2004, "In-tube cooling heat transfer of supercritical carbon dioxide. Part 1. Experimental measurement," International Journal of Refrigeration, **27**(7), pp. 736–747.

[19] Cabeza, L. F., de Gracia, A., Fernández, A. I., and Farid, M. M., 2017, "Supercritical CO2 as heat transfer fluid: A review," Applied Thermal Engineering, **125**, pp. 799–810.

[20] Ehsan, M. M., Guan, Z., and Klimenko, A., 2018, "A comprehensive review on heat transfer and pressure drop characteristics and correlations with supercritical CO2 under heating and cooling applications," Renewable and Sustainable Energy Reviews, **92**, pp. 658–675.

[21] Fan, Y., Tang, G., Li, X., Yang, D., and Wang, S., 2019, "Correlation evaluation on circumferentially average heat transfer for supercritical carbon dioxide in non-uniform heating vertical tubes," Energy, **170**, pp. 480–496.

[22] Xie, J., Liu, D., Yan, H., Xie, G., and Boetcher, S. K., 2020, "A review of heat transfer deterioration of supercritical carbon dioxide flowing in vertical tubes: Heat transfer behaviors, identification methods, critical heat fluxes, and heat transfer correlations," International Journal of Heat and Mass Transfer, **149**, p. 119233.

[23] Bodkha, K. and Maheshwari, N. K., 2021, "Heat Transfer in Supercritical Fluids: A Review," Journal of Nuclear Engineering and Radiation Science, **7**(3).

[24] Bringer, R. and Smith, J., 1957, "Heat Transfer in the Critical Region," AlChE, **3**(1), pp. 49–55.

[25] Gupta, S., Saltanov, E., Mokry, S. J., Pioro, I., Trevani, L., and McGillivray, D., 2013, "Developing empirical heat-transfer correlations for supercritical CO2 flowing in vertical bare tubes," Nuclear Engineering and Design, **261**, pp. 116–131.

[26] Saltanov, E., Pioro, I., and Harvel, G., 2013, "Preliminary Investigation of Heat-Transfer Correlation for Upward Flow of CO2 at Supercritical Pressure," *Volume 6 Beyond Design Basis Events Student Paper Competition*, American Society of Mechanical Engineers, doi: 10.1115/icone21-16399.

[27] Petukhov, B. S. and Kirillov, V. V., 1958, "About Heat Transfer at Turbulent Fluid Flow in Tubes (in Russian)," Thermal Engineering, (4), pp. 63–68.

[28] Filonenko, G. K., 1954, "Hydraulic Resistance in Pipes (in Russian)," Teploenergetika, **1**(4), pp. 40–44.

[29] Jackson, J. D. and Hall, W. B., 1979, *Turbulent Forced Convection in Channels and Bundles: Theory and Applications to Heat Exchangers and Nuclear Reactors*, Vol. 2, Hemisphere Publishing Corporation, New York, Chap. Forced Convection Heat Transfer to Fluids at Supercritical Pressure, pp. 563–612.

[30] McAdams, W. H., 1942, *Heat Transmission*, 2nd ed., Vol. 10, McGraw-Hill Book Company, New York and London.

[31] Prandtl, L., 1949, *Fuhrer durch die Stromungslehre (Guide to Flow Theory)*, Vieweg und Sohn, Braunschweig.

[32] Gnielinski, V., 1976, "New equations for heat and mass transfer in turbulent pipe and channel flow," International Journal of Chemical Engineering, **16**(2), pp. 359–368.

[33] Petukhov, B., 1970, *Advances in Heat Transfer*, Vol. 6, Academic Press, San Diego, CA, Chap. Heat transfer and friction in turbulent pipe flow with variable physicals properties,

Journal of Heat Transfer. Received April 07, 2022;
Accepted manuscript posted August 25, 2022. doi:10.1115/1.4055345

pp. 503–564.

[34] Krasnoshchekov, E. and Protopopov, V., 1960, "About heat transfer in flow of carbon dioxide and water at supercritical region of state parameters," Thermal Engineering, **29**(10), p. 94.

[35] Swenson, H. S., Carver, J. R., and Kakarala, C. R., 1965, "Heat Transfer to Supercritical Water in Smooth-Bore Tubes," J of Heat Transfer-Transactions of the ASME, **87**(4), pp. 477–483.

[36] Petukhov, B. S., Krasnoshchekov, E. A., and Protopopov, V. S., 1961, "An Investigation of Heat Transfer to Fluids Flowing in Pipes Under Supercritical Conditions," Paper No. 67, pp. 569–578.

[37] Petukhov, B. and Popov, V., 1963, "Theoretical calculation of heat exchange and frictional resistance in turbulent flow in tubes of an incompressible fluid with thermophysical properties," High Temperature, **1**(1), pp. 69–83.

[38] Krasnoshchekov, E. and Protopopov, V., 1966, "Experimental Study of Heat Exchange in Carbon Dioxide in the Supercritical Range at High Temperature Drops," High Temperature, **1**, pp. 375–382.

[39] Krasnoshchekov, E., Kuraeva, I., and Protopopov, V., 1970, "Local Heat transfer of Carbon Dioxide at Supercritical Pressure Under Cooling Conditions," High Temperature, **7**(5), pp. 922–930.

[40] Krasnoshchekov, E. and Protopopov, V., 1972, "A Generalized Relationship for Calculation of Heat Transfer to Carbon Dioxide at Supercritical Pressure," High Temperature, **6**(9), pp. 1215–1219.

[41] Krasnoshchekov, E., Protopopov, V., Parkhovnik, I., and Silin, V., 1972, "Some Results of an Experimental Investigation of Heat Transfer to Carbon Dioxide at Supercritical Pressure and Temperature Heads of up to 850 C," High Temperature, **9**(5), pp. 992–995.

[42] Petukhov, B., Kurganov, V., and Gladuntsov, A., 1973, "Heat transfer in turbulent pipe flow of gases with variable properties," Heat Transfer - Soviet Research, **5**(4), pp. 109–116.

[43] Protopopov, V., 1977, "Generalizing Relations for the Local Heat-Transfer Coefficients Turbulent Flows of Water and Carbon Dioxide at Supercritical Pressure in a Uniform Heated Circular Tube," High Temperature, **15**(4), pp. 687–692.

[44] Baskov, V., Kuraeva, I., and Protopopov, V., 1977, "Heat transfer with the turbulent flow of a liquid at supercritical pressure intubes under cooling conditions," High Temperature, **15**(1), pp. 81–86.

[45] Jackson, J. D. and Hall, W. B., 1979, *Turbulent Forced Convection in Channels and Bundles: Theory and Applications to Heat Exchangers and Nuclear Reactors*, Vol. 2, Hemisphere Publishing Corporation, New York, Chap. Influences of Buoyancy on Heat Transfer to Fluids Flowing in Vertical Tubes Under Turbulent Conditions, pp. 613–640.

[46] Watts, M. and Chou, C., 1982, "Mixed convection heat transfer to supercritical pressure water," Paper No. MC16, pp. 495–500.

[47] Petrov, N. and Popov, V., 1985, "Heat-transfer and resistance of carbon-dioxide being cooled in the supercritical region," Thermal Engineering, **32**(3), pp. 131–134.

[48] Ghajar, A. J. and Asadi, A., 1986, "Improved forced convective heat-transfer correlations for liquids inthe near-critical region," AIAA Journal, **24**(12), pp. 2030–2037.

[49] Petrov, N. and Popov, V., 1988, "Heat-transfer and hydraulic resistance with turbulent-flow

Journal of Heat Transfer. Received April 07, 2022;
Accepted manuscript posted August 25, 2022. doi:10.1115/1.4055345

in a tube of water at supercritical parameters of state," Thermal Engineering, **35**(10), pp. 577–580.

[50] Olson, D. A., 1999, "Heat Transfer of Supercritical Carbon Dioxide Flowing in a Cooled Horizontal Tube," National Institute of Standards and Technology, Gaithersburg, MD USA, Tech. Rep. NISTIR 6496.

[51] Fang, X., 1999, "Modeling and Analysis of Gas Coolers," Department of Mechanical and Industrial Engineering, University of Illinois at Urbana Champaign, USA.

[52] Pitla, S. S., Groll, E. A., and Ramadhyani, S., 2002, "New correlation to predict the heat transfer coefficient during in-tube cooling of turbulent supercritical CO2," International Journal of Refrigeration, **25**(7), pp. 887–895.

[53] Liao, S. M. and Zhao, T. S., 2002, "Measurements of Heat Transfer Coefficients From Supercritical Carbon Dioxide Flowing in Horizontal Mini/Micro Channels," J of Heat Transfer-Transactions of the ASME, **124**(3), pp. 413–420.

[54] Dittus, F. and Boelter, L., 1930, "Heat Transfer in Automobile Radiators of the Tubular Type," Publications of Engineering, **2**, p. 443.

[55] Winterton, R., 1998, "Where did the Dittus and Boelter equation come from?" International Journal of Heat and Mass Transfer, **41**(4-5), pp. 809–810.

[56] Williams, W. C., 2011, "If the Dittus and Boelter equation is really the McAdams equation, then should not the McAdams equation really be the Koo equation?" International Journal of Heat and Mass Transfer, **54**(7-8), pp. 1682–1683.

[57] Liao, S. and Zhao, T., 2002, "An experimental investigation of convection heat transfer to supercritical carbon dioxide in miniature tubes," International Journal of Heat and Mass Transfer, **45**(25), pp. 5025–5034.

[58] Yoon, S. H., Kim, J. H., Hwang, Y. W., Kim, M. S., Min, K., and Kim, Y., 2003, "Heat transfer and pressure drop characteristics during the in-tube cooling process of carbon dioxide in the supercritical region," International Journal of Refrigeration, **26**(8), pp. 857–864.

[59] Chao, Y., Lopes, N. C., Ricklick, M. A., and Boetcher, S. K. S., 2021, "Effect of the Heat Transfer Coefficient Reference Temperatures on Validating Numerical Models of Supercritical CO2," Journal of Verification, Validation and Uncertainty Quantification, **6**(4).

[60] Son, C.-H. and Park, S.-J., 2006, "An experimental study on heat transfer and pressure drop characteristics of carbon dioxide during gas cooling process in a horizontal tube," International Journal of Refrigeration, **29**(4), pp. 539–546.

[61] Huai, X. and Koyama, S., 2007, "Heat Transfer Characteristics of Supercritical CO2 Flow in Small-Channeled Structures," Experimental Heat Transfer, **20**(1), pp. 19–33.

[62] Kim, J. K., Jeon, H. K., and Lee, J. S., 2007, "Wall temperature measurement and heat transfer correlation of turbulent supercritical carbon dioxide flow in vertical circular/non-circular tubes," Nuclear Engineering and Design, **237**(15-17), pp. 1795–1802.

[63] Kuang, G., Ohadi, M., and Dessiatoun, S., 2008, "Semi-Empirical Correlation of Gas Cooling Heat Transfer of Supercritical Carbon Dioxide in Microchannels," HVAC&R Research, **14**(6), pp. 861–870.

[64] Kim, H., Bae, Y. Y., Kim, H. Y., Song, J. H., and Cho, B. H., 2008, "Experimental Investigation on the Heat Transfer Characteristics in Upward Flow of Supercritical Carbon Dioxide," Nuclear Technology, **164**(1), pp. 119–129.

[65] Bae, Y.-Y. and Kim, H.-Y., 2009, "Convective heat transfer to CO2 at a supercritical pressure flowing vertically upward in tubes and an annular channel," Experimental Thermal and Fluid Science, **33**(2), pp. 329–339.

[66] Bruch, A., Bontemps, A., and Colasson, S., 2009, "Experimental investigation of heat transfer of supercritical carbon dioxide flowing in a cooled vertical tube," International Journal of Heat and Mass Transfer, **52**(11-12), pp. 2589–2598.

[67] Bae, Y.-Y., Kim, H.-Y., and Kang, D.-J., 2010, "Forced and mixed convection heat transfer to supercritical CO2 vertically flowing in a uniformly-heated circular tube," Experimental Thermal and Fluid Science, **34**(8), pp. 1295–1308.

[68] Li, Z.-H., Jiang, P.-X., Zhao, C.-R., and Zhang, Y., 2010, "Experimental investigation of convection heat transfer of CO2 at supercritical pressures in a vertical circular tube," Experimental Thermal and Fluid Science, **34**(8), pp. 1162–1171.

[69] Oh, H.-K. and Son, C.-H., 2010, "New correlation to predict the heat transfer coefficient in-tube cooling of supercritical CO2 in horizontal macro-tubes," Experimental Thermal and Fluid Science, **34**(8), pp. 1230–1241.

[70] Kim, D. E. and Kim, M. H., 2010, "Experimental study of the effects of flow acceleration and buoyancy on heat transfer in a supercritical fluid flow in a circular tube," Nuclear Engineering and Design, **240**(10), pp. 3336–3349.

[71] Kim, D. E. and Kim, M.-H., 2011, "Experimental investigation of heat transfer in vertical upward and downward supercritical CO2 flow in a circular tube," International Journal of Heat and Fluid Flow, **32**(1), pp. 176–191.

[72] Kim, D. E. and Kim, M. H., 2011, "Two layer heat transfer model for supercritical fluid flow in a vertical tube," The Journal of Supercritical Fluids, **58**(1), pp. 15–25.

[73] Bae, Y. Y., 2011, "Mixed convection heat transfer to carbon dioxide flowing upward and downward in a vertical tube and an annular channel," Nuclear Engineering and Design, **241**(8), pp. 3164–3177.

[74] Mokry, S. J. and Pioro, I. L., 2011, "Heat Transfer Correlation for Supercritical Carbon DioxideFlowing Upward in a Vertical Bare Tube," *Supercritical CO2 Power Cycle Symposium*.

[75] Preda, T., Saltanov, E., Pioro, I., and Gabriel, K. S., 2012, "Development Of A Heat Transfer Correlation For Supercritical CO2 Based OnMultiple Data Sets," *Proceedings of the 2012 20th International Conference on Nuclear Engineering*.

[76] Liu, Z.-B., He, Y.-L., Yang, Y.-F., and Fei, J.-Y., 2014, "Experimental study on heat transfer and pressure drop of supercritical CO2 cooled in a large tube," Applied Thermal Engineering, **70**(1), pp. 307–315.

[77] Saltanov, E., Pioro, I., Mann, D., Gupta, S., Mokry, S., and Harvel, G., 2015, "Study on Specifics of Forced-Convective Heat Transfer in Supercritical Carbon Dioxide," Journal of Nuclear Engineering and Radiation Science, **1**(1).

[78] Saltanov, E., 2015, "Specifics of Forced-Convective Heat Transfer to Supercritical CO2 Flowing Upward in Vertical Bare Tubes," Ph.D. thesis, University of Ontario Institute of Technology.

[79] Ma, T., xiao Chu, W., yang Xu, X., tung Chen, Y., and wang Wang, Q., 2016, "An experimental study on heat transfer between supercritical carbon dioxide and water near the

Journal of Heat Transfer. Received April 07, 2022;
Accepted manuscript posted August 25, 2022. doi:10.1115/1.4055345

pseudo-critical temperature in a double pipe heat exchanger," International Journal of Heat and Mass Transfer, **93**, pp. 379–387.

[80] Yang, M., 2016, "Numerical study of the heat transfer to carbon dioxide in horizontal helically coiled tubes under supercritical pressure," Applied Thermal Engineering, **109**, pp. 685–696.

[81] Liu, G., Huang, Y., Wang, J., and Leung, L. H., 2016, "Heat transfer of supercritical carbon dioxide flowing in a rectangular circulation loop," Applied Thermal Engineering, **98**, pp. 39–48.

[82] Liu, S., Huang, Y., Liu, G., Wang, J., and Leung, L. K., 2017, "Improvement of buoyancy and acceleration parameters for forced and mixed convective heat transfer to supercritical fluids flowing in vertical tubes," International Journal of Heat and Mass Transfer, **106**, pp. 1144–1156.

[83] Zhang, G.-W., Hu, P., Chen, L.-X., and Liu, M.-H., 2018, "Experimental and simulation investigation on heat transfer characteristics of in-tube supercritical CO2 cooling flow," Applied Thermal Engineering, **143**, pp. 1101–1113.

[84] Chao, Y., Lopes, N. C., Ricklick, M. A., and Boetcher, S. K. S., 2022, "Hydraulic development length and boundary condition effects on local sCO2 heat transfer coefficients," *The 7th International Supercritical CO2 Power Cycles Symposium*, San Antonio, Texas.

[85] Zhang, Q., Li, H., Kong, X., Liu, J., and Lei, X., 2018, "Special heat transfer characteristics of supercritical CO2 flowing in a vertically-upward tube with low mass flux," International Journal of Heat and Mass Transfer, **122**, pp. 469–482.

[86] Fan, Y. and Tang, G., 2018, "Numerical investigation on heat transfer of supercritical carbon dioxide in a vertical tube under circumferentially non-uniform heating," **138**, pp. 354–364.

[87] Kim, T. H., Kwon, J. G., Park, J. H., Park, H. S., and Kim, M. H., 2019, "Heat transfer model for horizontal flows of CO2 at supercritical pressures in terms of mixed convection," International Journal of Heat and Mass Transfer, **131**, pp. 1117–1128.

[88] Wang, J., Guan, Z., Gurgenci, H., Veeraragavan, A., Kang, X., and Hooman, K., 2019, "A computationally derived heat transfer correlation for in-tube cooling turbulent supercritical CO2," International Journal of Thermal Sciences, **138**, pp. 190–205.

[89] Zhang, S., Xu, X., Liu, C., Liu, X., and Dang, C., 2019, "Experimental investigation on the heat transfer characteristics of supercritical CO2 at various mass flow rates in heated vertical-flow tube," Applied Thermal Engineering, **157**.

[90] Zhang, S., Xu, X., Liu, C., Liu, X., Ru, Z., and Dang, C., 2020, "Experimental and numerical comparison of the heat transfer behaviors and buoyancy effects of supercritical CO2 in various heating tubes," International Journal of Heat and Mass Transfer, **149**, p. 119074.

[91] Polyakov, A., 1974, "Development of secondary free-convection currents in forced turbulent flow in horizontal tubes," Journal of Applied Mechanics and Technical Physics, **15**(5), pp. 632–637.

[92] Guo, P., Liu, S., Yan, J., Wang, J., and Zhang, Q., 2020, "Experimental study on heat transfer of supercritical CO2 flowing in a mini tube under heating conditions," International Journal of Heat and Mass Transfer, **153**, p. 119623.

[93] Liu, X., Xu, X., Liu, C., Zhang, S., He, J., and Dang, C., 2020, "Flow structure at different stages of heat transfer deterioration with upward, mixed turbulent flow of supercritical CO2

Journal of Heat Transfer. Received April 07, 2022;
Accepted manuscript posted August 25, 2022. doi:10.1115/1.4055345

heated in vertical straight tube," Applied Thermal Engineering, **181**, p. 115987.

[94] Zhu, B., Xu, J., Yan, C., and Xie, J., 2020, "The general supercritical heat transfer correlation for vertical up-flow tubes: K number correlation," International Journal of Heat and Mass Transfer, **148**, p. 119080.

[95] Wang, L., Pan, Y. C., Lee, J. D., Wang, Y., Fu, B.-R., and Pan, C., 2020, "Experimental investigation in the local heat transfer of supercritical carbon dioxide in the uniformly heated horizontal miniature tubes," International Journal of Heat and Mass Transfer, **159**, p. 120136.

[96] Wang, L., Pan, Y. C., Lee, J. D., Fu, B.-R., and Pan, C., 2021, "Convective heat transfer characteristics of supercritical carbon dioxide in vertical miniature tubes of a uniform heating experimental system," International Journal of Heat and Mass Transfer, **167**, p. 120833.

[97] Wahl, A., Mertz, R., Laurien, E., and Starflinger, J., 2021, "Heat transfer correlation for sCO2 cooling in a 2 mm tube," The Journal of Supercritical Fluids, **173**, p. 105221.

[98] Viswanathan, K. and Krishnamoorthy, G., 2021, "The effects of wall heat fluxes and tube diameters on laminar heat transfer rates to supercritical CO2," International Communications in Heat and Mass Transfer, **123**, p. 105197.

[99] Wang, P., Ding, P., Li, W., Xie, R., Duan, C., Hong, G., and Zhang, Y., 2021, "Experimental study on heat transfer characteristics of supercritical carbon dioxide natural circulation," Nuclear Engineering and Technology.

[100] Yang, M., Li, G., Liao, F., Li, J., and Zhou, X., 2021, "Numerical study of characteristic influence on heat transfer of supercritical CO2 in helically coiled tube with non-circular cross section," International Journal of Heat and Mass Transfer, **176**, p. 121511.

[101] Yang, K.-T., 2008, "Artificial Neural Networks (ANNs): A New Paradigm for Thermal Science and Engineering," J of Heat Transfer-Transactions of the ASME, **130**(9).

[102] Hughes, M. T., Kini, G., and Garimella, S., 2021, "Status, Challenges, and Potential for Machine Learning in Understanding and Applying Heat Transfer Phenomena," J of Heat Transfer-Transactions of the ASME, **143**(12).

[103] Malekan, M., Khosravi, A., Goshayeshi, H. R., Assad, M. E. H., and Pabon, J. J. G., 2019, "Thermal Resistance Modeling of Oscillating Heat Pipes for Nanofluids by Artificial Intelligence Approach," J of Heat Transfer-Transactions of the ASME, **141**(7).

[104] Dawahdeh, A., Oh, J., Zhai, T., and Palazzolo, A., 2021, "Computational Fluid Dynamics—Machine Learning Prediction of Machinery Coupling Windage Heating and Power Loss," J of Heat Transfer-Transactions of the ASME, **143**(8).

[105] Smith, R. and Dutta, S., 2021, "Conjugate Thermal Optimization With Unsupervised Machine Learning," J of Heat Transfer-Transactions of the ASME, **143**(5).

[106] McClure, E. R. and Carey, V. P., 2021, "Genetic Algorithm and Deep Learning to Explore Parametric Trends in Nucleate Boiling Heat Transfer Data," J of Heat Transfer-Transactions of the ASME, **143**(12).

[107] Kang, M. and Kwon, B., 2021, "Deep Learning of Forced Convection Heat Transfer," J of Heat Transfer-Transactions of the ASME, **144**(2).

[108] Cai, S., Wang, Z., Wang, S., Perdikaris, P., and Karniadakis, G. E., 2021, "Physics-Informed Neural Networks for Heat Transfer Problems," J of Heat Transfer-Transactions of the ASME, **143**(6).

Journal of Heat Transfer. Received April 07, 2022;
Accepted manuscript posted August 25, 2022. doi:10.1115/1.4055345

[109] Scalabrin, G. and Piazza, L., 2003, "Analysis of forced convection heat transfer to supercritical carbon dioxide inside tubes using neural networks," International Journal of Heat and Mass Transfer, **46**(7), pp. 1139–1154.

[110] Olson, D. A. and Allen, D., 1998, "Heat Transfer in Turbulent Supercritical Carbon Dioxide Flowing in a Heated Horizontal Tube," National Institute of Standards and Technology, Gaithersburg, MD USA, Tech. Rep. NISTIR 6234.

[111] Chen, J., Wang, K.-P., and Liang, M.-T., 2005, "Predictions of heat transfer coefficients of supercritical carbon dioxide using the overlapped type of local neural network," International Journal of Heat and Mass Transfer, **48**(12), pp. 2483–2492.

[112] Pesteei, S. and Mehrabi, M., 2010, "Modeling of convection heat transfer of supercritical carbon dioxide in a vertical tube at low Reynolds numbers using artificial neural network," International Communications in Heat and Mass Transfer, **37**(7), pp. 901–906.

[113] Jiang, P.-X., Zhang, Y., Xu, Y.-J., and Shi, R.-F., 2008, "Experimental and numerical investigation of convection heat transfer of CO2 at supercritical pressures in a vertical tube at low Reynolds numbers," International Journal of Thermal Sciences, **47**(8), pp. 998–1011.

[114] Chu, X., Chang, W., Pandey, S., Luo, J., Weigand, B., and Laurien, E., 2018, "A computationally light data-driven approach for heat transfer and hydraulic characteristics modeling of supercritical fluids: From DNS to DNN," International Journal of Heat and Mass Transfer, **123**, pp. 629–636.

[115] Bae, Y.-Y., Kim, H.-Y., and Yoo, T. H., 2011, "Effect of a helical wire on mixed convection heat transfer to carbon dioxide in a vertical circular tube at supercritical pressures," International Journal of Heat and Fluid Flow, **32**(1), pp. 340–351.

[116] Kim, H. Y., Kim, H., Song, J. H., Cho, B. H., and Bae, Y. Y., 2007, "Heat Transfer Test in a Vertical Tube Using CO_2 at Supercritical Pressures," Journal of Nuclear Science and Technology, **44**(3), pp. 285–293.

[117] Mokry, S., Pioro, I., and Duffey, R., 2009, "Experimental heat transfer to supercritical CO_2 flowing upward in a bare vertical tube," *Proc SCCO2 Power Cycle Symp*.

[118] Cho, B.-H., Kim, Y.-I., and Bae, Y.-Y., 2009, "Prediction of a heat transfer to CO_2 flowing in an upward path at a supercritical pressure," Nuclear Engineering and Technology, **41**(7), pp. 907–920.

[119] Lei, X., Zhang, Q., Zhang, J., and Li, H., 2017, "Experimental and Numerical Investigation of Convective Heat Transfer of Supercritical Carbon Dioxide at Low Mass Fluxes," Applied Sciences, **7**(12), p. 1260.

[120] Song, J., Kim, H., Kim, H., and Bae, Y., 2008, "Heat transfer characteristics of a supercritical fluid flow in a vertical pipe," The Journal of Supercritical Fluids, **44**(2), pp. 164–171.

[121] Gupta, S., Saltanov, E., and Pioro, I., 2013, "Heat Transfer Correlation for Supercritical Carbon Dioxide Flowing in Vertical Bare Tubes," *Volume 6: Beyond Design Basis Events Student Paper Competition*, American Society of Mechanical Engineers, doi: 10.1115/icone21-16453.

[122] Zahlan, H., Groeneveld, D., and Tavoularis, S., 2015, "Measurements of convective heat transfer to vertical upward flows of CO2 in circular tubes at near-critical and supercritical pressures," Nuclear Engineering and Design, **289**, pp. 92–107.

[123] Jiang, K., 2015, "An Experimental Facility for Studying Heat Transfer in Supercritical Flu-

Journal of Heat Transfer. Received April 07, 2022;
Accepted manuscript posted August 25, 2022. doi:10.1115/1.4055345

ids," Master's thesis, University of Ottawa, doi:10.20381/RUOR-2760.

[124] Ye, K., Zhang, Y., Yang, L., Zhao, Y., Li, N., and Xie, C., 2019, "Modeling convective heat transfer of supercritical carbon dioxide using an artificial neural network," Applied Thermal Engineering, **150**, pp. 686–695.

[125] Kim, H.-Y., Kim, H.-R., Kang, D.-J., Song, J.-H., and Bae, Y.-Y., 2008, "Experimental investigations on heat transfer to CO_2 flowing upward in a narrow annulus at supercritical pressures," Nuclear Engineering and Technology, **40**(2), pp. 155–162.

[126] Zhu, B., Zhu, X., Xie, J., Xu, J., and Liu, H., 2021, "Heat Transfer Prediction of Supercritical Carbon Dioxide in Vertical Tube Based on Artificial Neural Networks," Journal of Thermal Science, **30**(5), pp. 1751–1767.

[127] Lei, X., Zhang, J., Gou, L., Zhang, Q., and Li, H., 2019, "Experimental study on convection heat transfer of supercritical CO2 in small upward channels," Energy, **176**, pp. 119–130.

[128] Bishop, A. A., Sandberg, R. O., and Tong, L. S., 1964, "High-temperature supercritical pressure water loop Part IV: Forced convection heat transfer to water at near-critical temperatures and super-critical pressures," Westinghouse Electric Corp. Atomic Power Div., Pittsburgh, Tech. Rep. WCAP-2056.

[129] Mokry, S., Pioro, I., Farah, A., King, K., Gupta, S., Peiman, W., and Kirillov, P., 2011, "Development of supercritical water heat-transfer correlation for vertical bare tubes," Nuclear Engineering and Design, **241**(4), pp. 1126–1136.

[130] Yu, J., Jia, B., Wu, D., and Wang, D., 2009, "Optimization of heat transfer coefficient correlation at supercritical pressure using genetic algorithms," Heat and Mass Transfer, **45**(6), pp. 757–766.

[131] Sun, F., Xie, G., and Li, S., 2021, "An artificial-neural-network based prediction of heat transfer behaviors for in-tube supercritical CO2 flow," Applied Soft Computing Journal, **102**, p. 107110.

[132] Sun, F., Xie, G., Song, J., Li, S., and Markides, C. N., 2021, "Thermal characteristics of in-tube upward supercritical CO2 flows and a new heat transfer prediction model based on artificial neural networks (ANN)," Applied Thermal Engineering, **194**, p. 117067.

[133] S, R. P. K., V, K., M, S. B., and Ponangi, B. R., 2022, "Turbulent Heat Transfer Characteristics of Supercritical Carbon Dioxide for a Vertically Upward Flow in a Pipe Using Computational Fluid Dynamics and Artificial Neural Network," J of Heat Transfer-Transactions of the ASME, **144**(1).

Journal of Heat Transfer. Received April 07, 2022;
Accepted manuscript posted August 25, 2022. doi:10.1115/1.4055345

Table 1 Parameters n, B, and k as a function of P/P_c for Eqs. (13) and (14) from [39].

P, bar	80	85	90	100	129	78.45
P/P_c	1.08	1.15	1.22	1.35	1.63	1.06
n	0.38	0.54	0.61	0.68	0.80	0.30
B	0.75	0.85	0.91	0.97	1.00	0.68
k	0.18	0.104	0.066	0.040	0	0.21

Table 2 Length correcting factor ϕ as a function of x/d for Eq. (22) from [42].

x/d	10	20	30	40	50	60	70	80	90	100	∞
ϕ	0.11	0.24	0.38	0.55	0.73	0.89	1.02	1.13	1.21	1.27	1.50

Table 3 Correcting factor φ(K) as a function of K for Eq. (26) from [43].

K	0.01	0.02	0.04	0.06	0.08	0.1	0.2	0.4
$\varphi(K)$	1	0.88	0.72	0.67	0.63	0.65	0.74	1

Journal of Heat Transfer. Received April 07, 2022;
Accepted manuscript posted August 25, 2022. doi:10.1115/1.4055345

Table 4 Exponents m and n as a function of P/P_c and $\overline{c}_p/c_{p,w}$ for Eq. (29) from [44].

Parameters	$\overline{c}_p/c_{p,w} > 1$			$\overline{c}_p/c_{p,w} < 1$		
P/P_c	1.07	1.35	1.63	1.08	1.35	1.63
m	1.2	1.6	1.6	0.45	0.45	0.45
n	0.15	0.1	0	0.15	0.10	0

Table 5 Constants c_1 - c_2, n_1 - n_6, and m_1 - m_6 for Eqs. (117)-(119) from [87].

Model	Position	c_1	n_1	n_2	n_3	n_4	n_5	n_6
Semi-empirical	Top	2.56	13/24	1/3	1/3	1/3	-2/3	1
	Bottom	4.06E-4						
	Position	c_2	m_1	m_2	m_3	m_4	m_5	m_6
	Top	9.89E2	-1/4	-3/20	-1/2	7/20	-3/20	-3/5
	Bottom	2.08						
Empirical	Position	c_1	n_1	n_2	n_3	n_4	n_5	n_6
	Top	1.14	-0.50	-0.36	0.54	0.83	-3.48E-14	0.52
	Bottom	0.11	-0.15	-0.41	0.26	0.54	-4.12E-04	0.63
	Position	c_2	m_1	m_2	m_3	m_4	m_5	m_6
	Top	7.05	-0.30	-0.55	-14.64	3.52E-6	-8.23E-11	-5.35
	Bottom	19.0	-0.33	-0.14	-0.40	3.98E-6	-3.55E-5	-0.88

Journal of Heat Transfer. Received April 07, 2022;
Accepted manuscript posted August 25, 2022. doi:10.1115/1.4055345

Table 6 1950s-1960s (Early Investigators) : boundary condition, flow direction, and operating range.

Author	Eq.	Boundary Condition	Flow Direction	Operating Range
Bringer & Smith [24]	(1)	heating	horizontal	$d = 4.57$ mm, $P = 8.27$ MPa, $Re_b = 3 \cdot 10^4 - 3 \cdot 10^5$, $q = 31.55 - 315.5$ kW/m^2, $T_b = 21 - 49$ °C
Petukhov & Kirillov [27]	(3)	heating, cooling	horizontal	$\mu_w/\mu_b = 0.08 - 40$, $Pr_b = 0.7 - 200$, $Re_b = 10^4 - 10^6$, subcritical
Krasnoshchekov & Protopopov [34]	(7)	heating	horizontal	$P = 8.3$ MPa, $Re_b = 2 \cdot 10^4 - 8.6 \cdot 10^5$, $Pr_b = 0.85 - 65$, $\mu_b/\mu_w = 0.90 - 3.60$, $k_b/k_w = 1 - 6$, $\bar{c}_p/c_{p,b} = 0.07 - 4.50$, $l/d > 15$
Petukhov & Popov [37]	(8)	–	horizontal	$Re = 10^4 - 5 \cdot 10^6$, $Pr = 0.5 - 2000$, subcritical
Swenson et al. [35]	(11)	heating	upward	$d = 9.42$ mm, $l = 1829$ mm, $P = 22.8 - 41.4$ MPa, $G = 542 - 2150$ kg/m^2·s, $T_w = 93 - 649$ °C, $T_b = 75 - 576$ °C
Krasnoshchekov & Protopopov [38]	(12)	heating	horizontal	$d = 4.08$ mm, $P/P_c = 1.06 - 1.33$, $T_b/T_{pc} = 0.9 - 1.2$, $T_w/T_{pc} = 0.9 - 2.5$, $Re_b = 8 \cdot 10^4 - 5 \cdot 10^5$, $Pr_b = 0.85 - 65$, $\rho_w/\rho_b = 0.09 - 1.0$, $\bar{c}_p/c_{p,b} = 0.02 - 4.0$, $q = 4.6 \cdot 10^4 - 2.6 \cdot 10^6$ W/m^2, $l/d \geq 15$

Table 7 1970s-1980s : boundary condition, flow direction, and operating range.

Author	Eq.	Boundary Condition	Flow Direction	Operating Range
Krasnoshchekov et al. [39]	(13)	cooling	horizontal	$P = 8$, 10, and 12 MPa, $T_b/T_{pc} = 0.999 - 1.53$, $T_w/T_{pc} = 0.901 - 1.19$, $d = 2.22$ mm, $l = 150$ mm
Krasnoshchekov & Protopopov [40]	(15)	heating	horizontal	same as Eq. (12), with new pressure range: $P/P_c = 1.02 - 5.25$
Krasnoshchekov et al. [41]	(17)	heating	horizontal	$d = 2.05$ mm, $l/d = 46.3$, $P/P_c = 1.35 - 1.42$, $Re_b = 0.6 \cdot 10^6 - 1.2 \cdot 10^6$, $Gr_b = 7.5 \cdot 10^6 - 15 \cdot 10^6$, $Gr_b/Re_b \approx 15$
Petukhov et al. [42]	(19)	–	horizontal	$Re = 4 \cdot 10^3 - 6 \cdot 10^5$, $Pr = 0.7 - 5 \cdot 10^5$, subcritical
Petukhov et al. [42]	(22)	–	horizontal	$Re_b > 7 \cdot 10^3$, $q^+ = 0.006 - 0.007$, $T_w/T_b < 4$, subcritical
Gnielinski [32]	(23)	–	horizontal	$Re = 2300 - 10^4$, subcritical
Gnielinski [32]	(24)	–	horizontal	$Re_b = 2300 - 10^6$, $Pr_b = 0.6 - 10^5$, subcritical
Protopopov [43]	(26)	heating	upward	–
Baskov et al. [44]	(29)	cooling	upward	$d = 4.12$ mm, $P = 8$, 10, and 12 MPa, $T_b = 17 - 212°C$, $T_w = 4 - 68$ °C, $G = 1560 - 4170$ kg / m^2·s
Jackson & Hall [29]	(30)-(32)	heating	horizontal	–

Journal of Heat Transfer. Received April 07, 2022;
Accepted manuscript posted August 25, 2022. doi:10.1115/1.4055345

Table 7 *continued.*

Author	Eq.	Boundary Condition	Flow Direction	Operating Range
Jackson & Hall [45]	(34)	heating	downward	–
Watts & Chou [46]	(35)	heating	upward, downward	$P = 25$ MPa, $T_b = 150 - 310$ °C, $G = 106 - 1060$ kg/m^2·s, $q = 175 - 440$ kW/m^2, $d = 25$ and 32.2 mm
Petrov & Popov [47]	(40)	cooling	horizontal, vertical	$P = 7.85$, 8, 10, and 12 MPa, $T_b = -7.5 - 203$ °C, $T_w = -30 - 130$ °C, $Re_b = 31 \cdot 10^3 - 800 \cdot 10^3$, $Re_w = 14 \cdot 10^3 - 790 \cdot 10^3$, $q = 0.14 \cdot 10^5 - 10 \cdot 10^5$ W/m^2, $G = 450 - 1000$ kg/m^2·s, $\rho_w/\rho_b = 1.1 - 6$, $\mu_w/\mu_b = 0.78 - 4.1$, $\bar{c}_p/c_{p,w} = 0.12 - 2.9$
Ghajar & Asadi [48]	(42)	heating	horizontal	developed using data from [36], [38], and [41]. Valid for $Re_b = 2 \cdot 10^4 - 1.2 \cdot 10^6$
Petrov & Popov [49]	(43)	cooling	–	for sCO_2, same as Eq. (40)

Table 8 1990s-2000s : boundary condition, flow direction, and operating range.

Author	Eq.	Boundary Condition	Flow Direction	Operating Range
Fang [51]	(45)	cooling	horizontal	$Re_w = 3000 - 10^6$, and $q/G = 0 - 350$ J/kg
Pitla et al. [52]	(48)	cooling	horizontal	$d = 4.72$ mm, $T_b = 20 - 124$ °C, $\dot{m} = 0.020 - 0.039$ kg/s, $P = 9.4 - 13.4$ MPa
Liao & Zhao [53]	(50)	cooling	horizontal	$P = 7.4 - 12$ MPa, $T_b = 20 - 110$ °C, $(T_b - T_w) = 2 - 30$ °C, $\dot{m} = 0.02 - 0.2$ kg/min, $Ri_b = 10^{-5} - 10^{-2}$, $d = 0.5 - 2.16$ mm
Liao & Zhao [57]	(52)-(54)	heating	horizontal, upward, downward	$d = 0.70 - 2.16$ mm, $P = 7.4 - 12$ MPa, $T_b = 20 - 110$ °C, $T_w - T_b = 2 - 30$ °C, $\dot{m} = 0.02 - 0.2$ kg/min. Eq. (52) valid for $Ri_b = 10^{-5} - 10^{-2}$. Eqs. (53)-(54) valid for $Bu = 2 \cdot 10^{-9} - 10^{-5}$
Yoon et al. [58]	(55)-(56)	cooling	horizontal	$d = 7.73mm$, $G_{CO_2} = 225 - 450$ kg/m^2·s, $P = 7.5 - 8.8$ MPa, $T_{b,in,CO_2} = 50 - 80$ °C, $\dot{m}_{H_2O} = 60 - 120$ g/s, and $T_{b,in,H_2O} = 7 - 12$ °C
Dang & Hihara [18]	(57)	cooling	horizontal	$d = 1 - 6$ mm, $l = 500$ mm, $P = 8 - 10$ MPa, $T_{b,in,CO_2} = 30 - 70$ °C, $G_{CO_2} = 200 - 1200$ kg/m^2·s, $q = 6 - 33$ kW/m^2
Son & Park [60]	(59)	cooling	horizontal	$d = 7.75$ mm, $l = 6000$ mm, $G_{CO_2} = 200 - 400$ kg/m^2·s, $T_{b,in,CO_2} = 90 - 100$ °C, $P = 7.5 - 10$ MPa
Huai & Koyama [61]	(60)	cooling	horizontal	$d = 1.31$ mm, $P = 7.4 - 8.5$ MPa, $T_b = 22 - 53$ °C, $G = 113.7 - 418.6$ kg/m^2·s, $q = 0.8 - 9$ kW/m^2

Journal of Heat Transfer. Received April 07, 2022;
Accepted manuscript posted August 25, 2022. doi:10.1115/1.4055345

Table 8 *continued.*

Author	Eq.	Boundary Condition	Flow Direction	Operating Range
Kim et al. [62]	(61)	heating	vertical	$l = 1200$ mm, $P = 8$ MPa, $T_{b,in} = 15 - 32$ °C, $q = 3 - 180$ kW/m^2, $G = 209 - 1230$ kg/m^2·s, $Re = 3 \cdot 10^4 - 1.4 \cdot 10^5$, $Gr_b = 5 \cdot 10^9 - 4 \cdot 10^{11}$. The circular, triangular, and square test sections had $d = 7.8$, 9.8, and 7.9 mm, respectively
Kuang et al. [63]	(66)	cooling	horizontal	$d = 0.5 - 2$ mm, $P = 8 - 10$ MPa, $G = 300 - 1200$ kg/m^2·s
Kim et al. [64]	(67)	heating	upward	$d = 4.4$ mm, $l = 2.1$ m, $P = 7.75 - 8.85$ MPa, $T_{b,in} = 5 - 30$ °C, $G = 400 - 1200$ kg/m^2·s, $q \leq 150$ kW/m^2
Bae & Kim [65]	(68)	heating	upward	$P = 7.75 - 8.85$ MPa, $T_{b,in} = 5 - 27$ °C, $G = 400 - 1200$ kg/m^2·s, and $q \leq 150$ kW/m^2. tubes: $d = 4.4$ and 9 mm, $l = 2.1$ and 2.65 m, respectively. annular channel: created between $d = 8$ mm heating rod and $d = 10$ mm tube, $l = 1.8$ m
Bruch et al. [66]	(70)-(71)	cooling	upward, downward	$d = 6$ mm, $l = 0.75$ m, $P = 7.4 - 12$ MPa, $T_{b,in,CO_2} = 15 - 70$ °C, $\dot{m}_{CO_2} = 5 - 60$ kg/hr, $G_{CO_2} = 50 - 590$ kg/m^2·s, $Re_b = 3600 - 1.8 \cdot 10^6$

Table 9 2010s-Present : boundary condition, flow direction, and operating range.

Author	Eq.	Boundary Condition	Flow Direction	Operating Range
Bae et al. [67]	(72)	heating	upward, downward	$d = 6.32$ mm, $l = 2.65$ m, $P = 7.75$ and 8.12 MPa, $T_{b,in} = 5 - 37$ °C, $G = 285 - 1200$ kg/m^2·s, $q = 30 - 170$ kW/m^2
Li et al. [68]	(76)	heating	upward, downward	$d = 2$ mm, $l = 290$ mm, $P = 7.8 - 9.5$ MPa, $T_{b,in} = 25 - 40$ °C, $q = 6.5 - 13.6$ kW/m^2, $Re_{in} = 3.8 \cdot 10^3 - 2 \cdot 10^4$
Oh & Son [69]	(79)	cooling	horizontal	$d = 4.55$ and 7.75 mm, $l = 4000$ and 6000 mm, $P = 7.5 - 10$ MPa, $G_{CO_2} = 200 - 600$ kg/m^2·s, $T_{b,in,CO_2} = 90 - 100$ °C
Kim & Kim [70]	(80)	heating	upward	$d = 4.5$ mm, $l = 900$ mm, $T_b = 29 - 115$ °C, $T_w = 41 - 238$ °C, $P = 7.46 - 10.26$ MPa, $q = 38 - 234$ kW/m^2, $G = 208 - 874$ kg/m^2·s, $Re_b = 18 \cdot 10^3 - 19 \cdot 10^4$, $Pr_b = 0.9 - 64$
Kim & Kim [71]	(83)	heating	upward, downward	same as Eq. (80)
Kim & Kim [72]	(84)	heating	upward	same as Eq. (80)
Bae [73]	(85)	heating	upward, downward	$P = 8.12$ MPa, $G = 400 - 1200$ kg/m^2·s, $q = 30 - 140$ kW/m^2, $T_{b,in} = 5 - 37$ °C. tube: $d = 4.57$ mm, $l = 2.25$ m. annular channel: created between $d = 8$ mm heating rod and $d = 10$ mm, $l = 1.8$ m

Journal of Heat Transfer. Received April 07, 2022;
Accepted manuscript posted August 25, 2022. doi:10.1115/1.4055345

Table 9 *continued.*

Author	Eq.	Boundary Condition	Flow Direction	Operating Range
Fang & Xu [16]	(88)	cooling	horizontal	developed using data from [39], [18], and [61]
Mokry & Pioro [74]	(93)	heating	upward	$d = 8$ mm, $l = 2.208$ m, $P = 7.6 - 8.8$ MPa, $G = 840 - 3000$ kg/m^2·s, $q \leq 600$ kW/m^2, $T_{b,in} = 20 - 40$ °C
Preda et al. [75]	(94)	heating	horizontal, vertical	$d = 0.948 - 9$ mm, $P = 7.58 - 9.58$ MPa, $G = 419 - 1200$ kg/m^2·s, $q = 20 - 130$ kW/m^2
Gupta et al. [25]	(95)-(97)	heating	upward	$d = 8$ mm, $l = 2.208$ m, $P = 7.57 - 8.8$ MPa, $G = 706 - 3169$ kg/m^2·s, $q = 9.3 - 616.6$ kW/m^2, $T_{b,in} = 20 - 40$ °C
Saltanov et al. [26]	(98)-(99)	heating	upward	developed using data from [64] for $d = 4.4$ mm and $P = 7.75$ MPa
Liu et al. [76]	(100)	cooling	horizontal	$d = 4 - 10.7$ mm, $P = 7.5 - 8.5$ MPa, $\dot{m} = 0.35 - 0.8$ kg/min, $T_{b,in} = 25 - 67$ °C
Saltanov et al. [77]	(101)	heating	upward	$d = 8.058$ mm, $P = 7.57 - 8.91$ MPa, $G = 674 - 3048$ kg/m^2·s, $q = 9.3 - 616$ kW/m^2, and $T_b = 20 - 161$ °C
Saltanov et al. [77]	(102)	heating	upward	$d = 4.4 - 8.1$ mm, $P = 7.57 - 8.91$ MPa, $G = 199 - 3048$ kg/m^2·s, $q = 9.9 - 616$ kW/m^2, $T_b = 5 - 161$ °C
Saltanov et al. [77]	(103)	heating	upward	$d = 8.1$ mm, $P = 7.57 - 8.85$ MPa, $G = 694 - 2987$ kg/m^2·s, $q = 180 - 616$ kW/m^2, $T_b = 22 - 35$ °C, and $T_w = 81 - 159$ °C
Saltanov [78]	(105)	heating	upward	$d = 8.1$ mm, $P = 7.58 - 8.91$ MPa, $T_b = 22 - 142$ °C, $T_w = 32$–223 °C, $G = 885$–3048 kg/m^2·s, $q = 27 - 616$ kW/m^2
Ma et al. [79]	(106)	cooling	–	$Re_b = 8 \cdot 10^4 - 4.9 \cdot 10^5$, $Pr_b = 11 - 130$
Yang [80]	(107)	cooling	horizontal	$d = 4$ mm, $P = 8 - 9$ MPa, $G = 150 - 350$ kg/m^2·s, $q = 30$ kW/m^2, $T_{b,in} = 346.15$ K
Liu et al. [81]	(108)	heating	vertical	$d = 4.4 - 10$ mm, $P = 7.44 - 8.86$ MPa, $G = 285 - 3059$ kg/m^2·s, $q = 29.3 - 537.2$ kW/m^2, $Re_b = 1.8 \cdot 10^4 - 1.17 \cdot 10^6$, $Pr_b = 0.77 - 10.3$
Liu et al. [82]	(109)	heating	upward, downward	$d = 6$ and 10 mm, $P = 7.4 - 10.6$ MPa, $G = 298.8 - 1506.5$ kg/m^2·s, $q = 4.7 - 296$ kW/m^2, $T_{b,in} = 16.4 - 49$ °C
Zhang et al. [83]	(112)-(113)	cooling	horizontal	$d = 4.12 - 9.44$ mm, $l = 1000$ mm, $P = 8 - 9$ MPa, $G = 160 - 240$ kg/m^2·s, $q = 34.5 - 105.4$ kW/m^2
Zhang et al. [85]	(114)	heating	upward	$d = 16$ mm, $P = 7.5 - 10.5$ MPa, $G = 50 - 200$ kg/m^2·s, $q = 5 - 60$ kW/m^2
Fan & Tang [86]	(115)	heating	upward	$d = 38$ mm, $P = 8.194 - 15$ MPa, $G = 1000 - 2000$ kg/m^2·s, $q_{max} = 100 - 400$ kW/m^2 (maximum heat flux on wall)
Fan et al. [21]	(116)	heating	upward	$d = 38$ mm, $P = 8.194$ MPa, $G = 2000 - 3000$ kg/m^2·s, $q_{max} = 0 - 537$ kW/m^2

Journal of Heat Transfer. Received April 07, 2022;
Accepted manuscript posted August 25, 2022. doi:10.1115/1.4055345

Table 9 *continued.*

Author	Eq.	Boundary Condition	Flow Direction	Operating Range
Kim et al. [87]	(117)	heating	horizontal	$d = 7.75$ mm, $l = 0.91$ m, $G = 104.34 - 391.91$ kg/m^2·s, $q = 5.1 - 26.9$ kW/m^2, $T_{b,in} = 13.8 - 30.1$ °C, $P = 7.586 - 7.614$ MPa
Wang et al. [88]	(121)	cooling	horizontal	$d = 15.75 - 24.36$ mm, $T_{b,in} = 25 - 65$ °C, $G = 243.6 - 800$ kg/m^2·s, $q = 5 - 36$ kW/m^2, $P = 8 - 10$ MPa, $Re = 7.7 \cdot 10^4 - 6.3 \cdot 10^5$, $Pr = 1.2 - 13.4$, $Ri = 3.1 \cdot 10^{-4} - 0.331$
Zhang et al. [89]	(123)	heating	upward, downward	$d = 4$ mm, $l = 1350$ mm, $P = 7.5 - 9$ MPa, $G = 80 - 400$ kg/m^2·s, $q = 10 - 62$ kW/m^2, $Bu < 10^{-4}$ (from Eq. (33))
Zhang et al. [90]	(126)-(128)	heating	horizontal	$d = 4$ mm, $l = 2000$ mm, $P = 7.5 - 9$ MPa, $\dot{m} = 80 - 600$ kg/m^{2}s, $q = 10 - 70$ kW/m^2
Guo et al. [92]	(130)	heating	horizontal	$d = 2$ mm, $P = 7.6 - 8.4$ MPa, $q = 100 - 200$ kW/m^2, $G = 400 - 700$ kg/m^2·s, $q/G = 250 - 500$ J/kg
Liu et al. [93]	(131)	heating	upward	$d = 4$ mm, $l = 2000$ mm, $P = 8$ MPa, $G = 278$ kg/m^2·s, $q = 15 - 35$ kW/m^2, $Re_{in} \geq 14 \cdot 10^3$
Zhu et al. [94]	(132)	heating	upward	$d = 2 - 26$ mm, $l = 290 - 2000$ mm, $P = 4.3 - 32$ MPa, $G = 315 - 2000$ kg/m^2·s, $q = 20 - 893$ kW/m^2
Wang et al. [95]	(134)	heating	horizontal	$d = 0.5 - 1$ mm, $P_{out} = 7.66 - 9$ MPa, $T_{b,in} = 30.8 - 37.3$ °C, $G = 672 - 4810$ kg/m^2·s, $q = 70.7 - 344.2$ kW/m^2
Wang et al. [96]	(136)	heating	upward	$d = 0.5 - 1$ mm, $P_{out} = 7.66 - 9$ MPa, $T_{b,in} = 30.8 - 37$ °C, $G = 672 - 4810$ kg/m^2·s, $q = 78.9 - 353.7$ kW/m^2
Wahl et al. [97]	(137)	cooling	horizontal	$d = 2$ mm, $l = 1200$ mm, $G = 400 - 1300$ kg/m^2·s, $P = 7.7 - 8.5$ MPa, $T_{b,co2} = 10 - 85$ °C, $T_{b,h2o} = 10 - 40$ °C
Viswanathan & Krishnamoorthy [98]	(138)	heating	horizontal	$d = 0.2 - 2$ mm, $q = 0.25 - 25$ kW/m^2, $Re_{in} = 40 - 400$, $T_{b,in} = 265$ °C, $P = 8.2$ MPa
Wang et al. [99]	(139)	heating	horizontal	$d = 7$mm, $l = 1500$ mm, $P = 7.58 - 10.26$ MPa, $T_{b,in} = 289.04 - 306.33$ K, $T_{b,out} = 294.59 - 382.57$ K, $q = 3.61 - 148.82$ kW/m^2, $G = 189.45 - 514.46$ kg/m^2·s, $V_{out} = 0.23 - 2.65$ m/s, $Re_{out} = 1.59 \cdot 10^4 - 1.66 \cdot 10^5$, $Pr = 0.72 - 14.29$

Journal of Heat Transfer. Received April 07, 2022;
Accepted manuscript posted August 25, 2022. doi:10.1115/1.4055345

Table 10 Input and output parameters used to predict sCO_2 thermal behavior, including relevant operating ranges.

Author		Output	Input	Operating Range
Scalabrin & Piazza [109]	1.)	Nu	Re, Pr, Ec	–
Chen et al. [111]	2.)	α	P_r, T_r, $\dot{m}$, q	
	3.)	Nu	Re, Pr, $\frac{\rho_w}{\rho_b}$, $\frac{\bar{c}_p}{c_{p,b}}$	
	4.)	α	P_r, T_r, $\dot{m}$, $\frac{T_w}{T_b}$	
Pesteei & Mehrabi [112]		α_x	Re, G, Bo^*, x^+, q	$q = 4.49 - 36.8$ kW/m^2, $Re_{in} = 1810 - 1993$, $T_{b,in}$ = 24.6 °C, and $P = 9.57$ MPa
Chu et al. [114]		T_w, τ_w	d, P, T_{in}, h_b, q	$d = 2, 5, 10$ mm, $q = 5, 10, 20, 30$ kW/m^2, $T_{in} = 15, 28$ °C, $P = 8, 8.8$ MPa
Ye et al. [124]		T_w	d, P, G, h_b, q	$d = 2 - 22$ mm, $T_b = -6 - 115$ °C, $P = 7.5 - 9.23$ MPa, $G = 100 - 3079$ kg/m^2·s, and $q = 0.479 - 616.3$ kW/m^2
Zhu et al. [126]				$d = 2 - 16$ mm, $P = 7.5 - 20.8$ MPa, $q = 5 - 350$ kW/m^2, and $G = 488 - 2000$ kg/m^2·s
Sun et al. [131]				$d = 4.4 - 22$ mm, $h_b = 183.5 - 537.8$ kJ/kg, $P = 7.5 - 9.23$ MPa, $G = 200 - 2000$ kg/m^2·s, and $q = 5 - 436$ kW/m^2
Sun et al. [132]	1.)	T_w	d, P, G, h_b, q	same as [131]
	2.)	α	Re_b, Re_w, Pr_b, Pr_w, $\frac{\rho_w}{\rho_b}$, $\frac{\mu_w}{\mu_b}$, $\frac{k_w}{k_b}$, $\frac{c_{p,w}}{c_{p,b}}$, $\frac{\bar{c}_p}{c_{p,b}}$	
Prasad et al. [133]		Nu	Re, Pr, Gr_q, q^+, $\frac{P}{P_c}$	$d = 3.5 - 9.5$ mm, $P = 76.21 - 100.5$ bar, $G = 238 - 1038$ kg/m^2·s, and $q = 26 - 250$ kW/m^2

Journal of Heat Transfer. Received April 07, 2022;
Accepted manuscript posted August 25, 2022. doi:10.1115/1.4055345

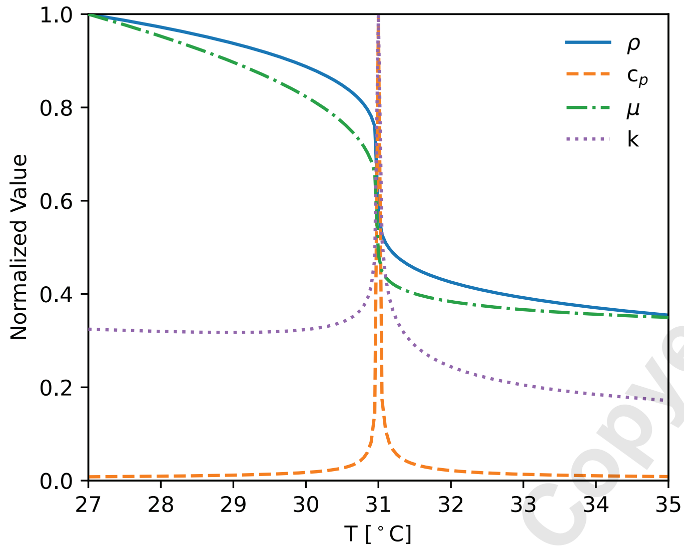

Fig. 1. Property variation of sCO_2 at P = 7.38 MPa.

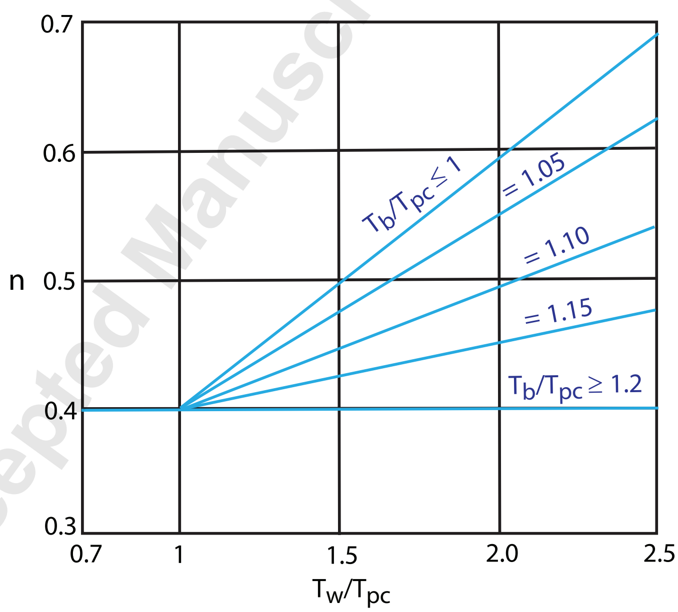

Fig. 2. Exponent n as a function of T_w/T_{pc} for Eq. (12) from [38].